Hindawi
International Journal of Energy Research
Volume 2024, Article ID 6029412, 22 pages
https://doi.org/10.1155/2024/6029412

Research Article

Opposing Mixed Convection Heat Transfer for Turbulent Single-Phase Flows

Kosuke Motegi[1], **Yasuteru Sibamoto**[1], **Takashi Hibiki**[2], **Naofumi Tsukamoto**[3] **and Junichi Kaneko**[3]

[1]*Nuclear Safety Research Center, Japan Atomic Energy Agency, 2-4 Shirakata, Tokai-mura, Naka-gun, Ibaraki 319-1195, Japan*
[2]*Department of Mechanical Engineering, City University of Hong Kong, 83 Tat Chee Avenue, Kowloon, Hong Kong*
[3]*Regulatory Standard and Research Department, Secretariat of Nuclear Regulation Authority, Roppongi First Building, 1-9-9 Roppongi, Minato-ku, Tokyo 106-8450, Japan*

Correspondence should be addressed to Yasuteru Sibamoto; sibamoto.yasuteru@jaea.go.jp
and Takashi Hibiki; thibiki@cityu.edu.hk

Received 7 August 2023; Revised 8 December 2023; Accepted 18 December 2023; Published 16 January 2024

Academic Editor: Guojun Yu

Convection, wherein forced and natural convections are prominent, is known as mixed convection. Specifically, when a forced convection flow is downward, this flow is called opposing flow. The objectives of this study are to gain a comprehensive understanding of opposing flow mixed convection heat transfer and to establish the prediction methodology by evaluating existing correlations and models. Several heat transfer correlations have been reported related to single-phase opposing flow; however, these correlations are based on experiments conducted in various channel geometries, working fluids, and thermal flow parameter ranges. Because the definition of nondimensional parameters and their validated range confirmed by experiments differ for each correlation reported in previous studies, establishing a guideline for deciding which correlation should be selected based on its range of applicability and extrapolation performance is important. This study reviewed the existing heat transfer correlations for turbulent opposing flow mixed convection and the single-phase heat transfer correlations implemented in the thermal–hydraulic system codes. Furthermore, the authors evaluated the predictive performance of each correlation by comparing them with the experimental data obtained under various experimental conditions. The Jackson and Fewster, Churchill, and Swanson and Catton correlations can accurately predict all the experimental data. The effect of the difference in the thermal boundary conditions, i.e., uniform heat flux and uniform wall temperature, on the turbulent mixed convection heat transfer coefficient is not substantial. The authors confirmed that heat transfer correlations using the hydraulic-equivalent diameter as a characteristic length can be used for predictions regardless of channel-geometry differences. Furthermore, correlations described based on nondimensional dominant parameters can be used for predictions regardless of the differences in working fluids. The authors investigated the extrapolation performance of the mixed convection heat transfer correlations for a wide range of nondimensional parameters and observed that the Jackson and Fewster, Churchill, and Aicher and Martin correlations exhibit excellent extrapolation performance with respect to natural and forced convection flows, indicating that they can be applied beyond the parameter range validated experimentally.

1. Introduction

The rapid cooling of a reactor pressure vessel (RPV) wall embrittled owing to exposure to neutrons could propagate cracks, if they exist, in the wall because of induced thermal stresses. This event is called pressurized thermal shock (PTS) and is one of the most severe loads that could act on a RPV wall. Loss of coolant accident (LOCA) in a pressurized water reactor (PWR) is the most important and commonly studied accident. During a LOCA, when the water inventory of the primary system decreases and water from the emergency core cooling system is supplied to the cold

leg (CL), the cooling water flows into the downcomer while mixing with the fluid in the CL and then cools the downcomer wall while further mixing with the surrounding water. Temperature distribution inside the downcomer wall needs to be determined to evaluate the thermal stress in the wall; therefore, the fluid bulk temperature and heat transfer coefficient need to be calculated. Depending on the accident scenario, the flow regime in the downcomer can be single-phase mixed convection, wherein forced and natural convections are equally prominent. Single-phase mixed convections are distinguished depending on the directions of forced convection. Mixed convection flowing downward along a heated wall like the downcomer is called an opposing flow. The heat transfer coefficient of turbulent opposing flow is more than that of forced convection because of the increased turbulence caused by the increased velocity gradient at the edge of the viscous sublayer next to a heated wall [1], thus requiring a proper evaluation.

Investigating PTS requires multidisciplinary analyses, including thermal–hydraulic analysis, probabilistic risk assessment, material analysis, and analysis based on fracture mechanics. Thermal–hydraulic analysis predicts the overcooling of the RPV wall accurately and effectively using thermal–hydraulic system codes. The thermal–hydraulic system codes can simulate the systems of nuclear plants and are indispensable for plant safety evaluation, where full-scale experiments cannot be realistically performed. Several countries independently developed their codes, including the reactor excursion and leak analysis program 5 (RELAP5) [2], transient reactor analysis code (TRAC) [3], TRAC/RELAP advanced computational engine (TRACE) [4], code for analysis of thermal–hydraulics during an accident of reactor and safety evaluation 3 (CATHARE-3) [5], analysis of thermal–hydraulics of leaks and transients (ATHLET) [6], multidimensional analysis of reactor safety KINS standard (MARS-KS) [7], and advanced multifluid analysis code for generation of thermal–hydraulic information (AMAGI) [8]. Among these codes, RELAP5 and TRACE are widely used for safety analysis and engineering design. The United States (US) Nuclear Regulatory Commission (NRC) and a consortium of countries and organizations that are members of the International Code Assessment and Applications Program (ICAP) and Code Applications and Maintenance Program (CAMP) jointly developed RELAP5. TRACE is the latest system analysis code that integrates the legacy safety analysis codes (TRAC–PF1 [9], TRAC–BF1 [10], and RELAP5 [2]) developed by the US NRC. RELAP5 and TRACE can choose the heat transfer correlation for a single-phase turbulent mixed convection developed by Swanson and Catton [11] to evaluate the heat transfer coefficient at a downcomer wall. The reactor integrity assessment method used for regulatory safety examination with respect to PTS events in Japan is based on the method prescribed in JEAC4206-2007 [12]. The JEAC4206-2007 uses the Jackson and Fewster correlation [13] to evaluate the heat transfer coefficient at the downcomer wall.

Heat transfer experiments related to mixed convection opposing flow have been conducted with respect to various channel geometries, working fluids, and thermal flow parameter ranges, and many correlations have been proposed. Because the correlations were represented using various dependent parameters comprising nondimensional parameters with different definitions, the mutual use of nondimensional experimental data and comparison among correlations were rarely conducted. When researchers and engineers apply correlations to their problems, establishing a guideline for deciding which correlations should be selected considering the range of applicability and extrapolation performance of the correlations is important. To derive reliable predictions with respect to the heat transfer coefficient under various conceivable accident scenarios, re-evaluating the existing experimental data and confirming the validity of the correlations against the experimental data under a wide range of thermal flow parameters is important.

The objectives of this study are to gain a comprehensive understanding of opposing flow mixed convection heat transfer and to establish the prediction methodology by evaluating existing correlations and models. This study is organized as follows. Section 2 reviews the existing heat transfer correlations related to opposing flow mixed convection and the wall heat transfer modeling for single-phase flows implemented in the thermal–hydraulic reactor system codes. Section 3 studies the applicability of the correlations with respect to the experiments using various channel geometries, working fluids, and thermal flow parameter ranges by comparing correlation predictions with experimental data. Section 4 studies the relationships among different dependent parameters with different definitions and compares the experimental data based on these relationships. Furthermore, this study investigates the extrapolation performance of the correlations over a wide range of nondimensional parameters. Section 5 summarizes the main results and presents our conclusions.

2. Existing Mixed Convection Heat Transfer Correlations

Figure 1 shows a mixed convection opposing flow with fluid flowing downward along a heated vertical plate. Figures 1(a) and 1(b) show velocity profiles for inertia-dominant and buoyancy-dominant conditions, respectively. Figure 1(c) shows a temperature profile. L is the length of the plate. The nondimensional numbers that appear in the nondimensionalized governing equations, the transport equations of heat and momentum approximated using the Boussinesq approximation, are the Reynolds number (Re), Grashof number (Gr), and Prandtl number (Pr).

$$\mathrm{Re} = \frac{l v_m}{\upsilon}, \tag{1a}$$

$$\mathrm{Gr} = \frac{g \beta (T_w - T_b) l^3}{\upsilon^2}, \tag{1b}$$

$$\mathrm{Pr} = \frac{\upsilon}{\alpha}, \tag{1c}$$

where l, v_m, υ, β, T_w, T_b, g, and α are the characteristic length, mean velocity, kinematic viscosity coefficient, thermal expansion coefficient, wall temperature, fluid bulk

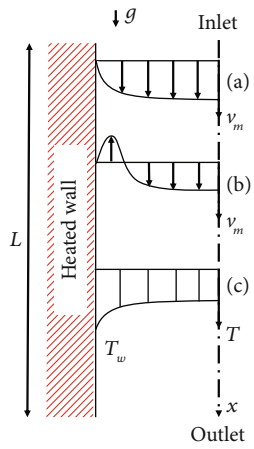

FIGURE 1: Schematics of velocity and temperature profiles of mixed convection opposing flow: (a) a velocity profile for inertia-dominant conditions, (b) a velocity profile for buoyancy-dominant conditions, and (c) a temperature profile.

temperature, gravitational acceleration, and thermal diffusivity, respectively. v_m is also termed as v_g for a gas and v_l for a liquid. The product of Gr and Pr gives the Rayleigh number (Ra), and the critical Ra indicates the criteria for transition from a laminar to turbulent natural convection flow.

$$\mathrm{Ra} = \mathrm{Gr}\,\mathrm{Pr}. \tag{2}$$

The nondimensionalized heat transfer coefficient h is the Nusselt number (Nu).

$$\mathrm{Nu} = \frac{h\,l}{k}, \tag{3}$$

where k is the thermal conductivity of a fluid. The averaged value $\bar{\mathrm{Nu}}$ over the channel length is frequently used when h varies along the streamline direction. Table 1 lists the channel geometries, the working fluids, and the dependent parameters used in previous experiments, on which the heat transfer correlations are based. Figure 2 shows the schematics of the channel geometries used in the experiments. Table 2 lists the nondimensional number ranges in which each correlation was validated based on the experimental data. The authors extracted these ranges from each of the references and summarized them in the table. The dependent parameters represent the heat transfer coefficient, depending on multiple parameters, in a simple equation. The dependent parameter increases as natural convection prevails and approaches zero as forced convection prevails. The subscripts b, w, and f are related to the reference temperature. A physical parameter with the subscripts b, w, and f is evaluated based on fluid bulk, wall, and mean boundary layer temperatures, respectively. Herein, the mean boundary layer temperature defined as $T_f = (T_w + T_b)/2$ is termed the film temperature. Researchers use different definitions of Gr, as follows:

$$\mathrm{Gr}_q = \frac{g\,\beta\,l^4\,q''_w}{\nu^2\,k} = \mathrm{Nu}\,\mathrm{Gr}, \tag{4}$$

where q''_w is the wall heat flux.

$$\overline{\mathrm{Gr}} \equiv \frac{(\rho_b - \bar{\rho})\,\rho_b\,g\,l^3}{\mu_b^2}, \tag{5}$$

where μ_b is the dynamic viscosity. The integrated mean density $\bar{\rho}$ is defined as

$$\bar{\rho} = \frac{1}{T_w - T_b}\int_{T_b}^{T_w} \rho\,dT. \tag{6}$$

The physical meanings of different Gr are detailed in the following sections.

2.1. Vertical Tube

2.1.1. Churchill. Churchill [14] proposed the interpolation formula expressed in Eq. (7) to determine the turbulent mixed convection heat transfer coefficient using the turbulent natural $\mathrm{Nu}_{\mathrm{nt}}$ and turbulent forced convection heat transfer correlation $\mathrm{Nu}_{\mathrm{ft}}$.

$$\bar{\mathrm{Nu}} = \left(\mathrm{Nu}_{\mathrm{ft}}^3 + \mathrm{Nu}_{\mathrm{nt}}^3\right)^{1/3}. \tag{7}$$

This expression is frequently used to determine mixed convection heat transfer coefficients [17]. To calculate $\mathrm{Nu}_{\mathrm{ft}}$, the Churchill correlation [18] developed for a circular tube is used.

$$\mathrm{Nu}_{\mathrm{ft}} = \frac{0.0357\ \mathrm{Re}\ \mathrm{Pr}^{1/3}\left(1 + \mathrm{Pr}^{-4/5}\right)^{-5/6}}{\ln\left(\mathrm{Re}/7\right)}. \tag{8}$$

The experimentally validated range of Eq. (8) is $0.02 \le \mathrm{Pr} \le 9810$. To calculate $\mathrm{Nu}_{\mathrm{nt}}$, the Churchill and Chu correlation [19] developed for a vertical plate is used.

$$\mathrm{Nu}_{\mathrm{nt}} = 0.15\mathrm{Ra}^{1/3}\left\{1 + \left(\frac{0.492}{\mathrm{Pr}}\right)^{9/16}\right\}^{-16/27}. \tag{9}$$

Churchill showed that Eq. (7) effectively predicts data with respect to the experiment conducted by Herbert and Sterns [20] for the mixed convection opposing flow in a vertical pipe with uniform wall temperature. Figure 2(a) depicts a typical experimental setup using a vertical tube. Herbert and Sterns conducted experiments on mixed convection aiding and opposing flows in a heated circular pipe with an inner diameter of 2.23 cm and a length of 183 cm. The working fluid used was water. The thermal boundary condition with respect to the wall was the uniform wall temperature (UWT) condition. All physical properties comprising the nondimensional numbers were evaluated at a film temperature. Because Eq. (7) asymptotically approaches Eq. (8) under forced convection-dominant conditions and Eq. (9) under natural convection-dominant conditions, Eq. (7) can be used for a wide range of

Table 1: Existing heat transfer correlations for mixed convection opposing flow.

Reference	Channel geometry	Fluid	Dependent parameter
Churchill (Eq. (7)) [14]	Tube	Water	—
Jackson and Fewster (Eq. (15)) [13]	Tube	Water	$\dfrac{\overline{\mathrm{Gr}}}{\mathrm{Re}_b^{2.625}\,\mathrm{Pr}_b^{0.5}}$
Aicher and Martin (Eq. (19)) [1]	Tube	Water	$\dfrac{\mathrm{Ra}_f^{0.333}}{\mathrm{Re}_b^{0.8}\,\mathrm{Pr}_b^{0.4}}$
Swanson and Catton (Eq. (24)) [11]	Rectangular duct	Freon-113	$\dfrac{\mathrm{Gr}_b}{\mathrm{Re}_b^2}$
Swanson and Catton (Eq. (30)) [15]	Rectangular duct	Freon-113	$\dfrac{\mathrm{Gr}_b}{\mathrm{Re}_b^{2.6}\left(\mathrm{Pr}_b^{0.5}+1\right)}$
P. Poskas and R. Poskas (Eq. (33)) [16]	Rectangular duct	Air	$\dfrac{\mathrm{Gr}_q}{\mathrm{Re}_b^{2.5}\,\mathrm{Pr}_b^{0.8}}$

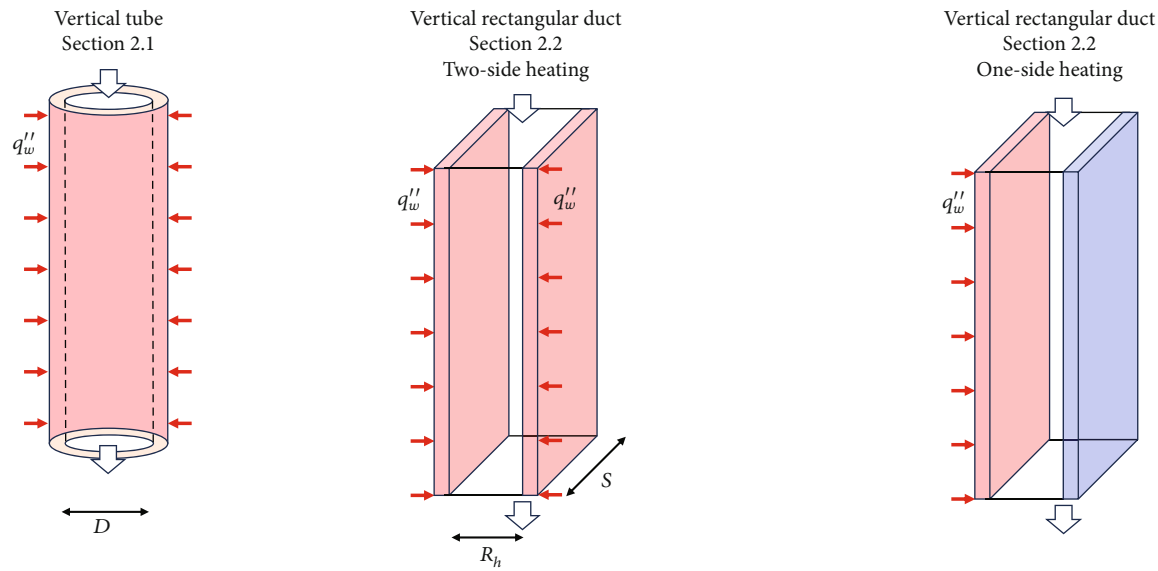

(a) Vertical tube (Section 2.1) (b) Vertical rectangular duct (Section 2.2), two-side heating (c) Vertical rectangular duct (Section 2.2), one-side heating

Figure 2: Schematics of the channel geometries for (a) a vertical tube and (b) two-side and (c) one-side heating vertical rectangular ducts. q''_w is the wall heat flux. D is the inner diameter of a tube. R_h and S are the gap and the width of a rectangular duct.

Table 2: Ranges of nondimensional numbers for which the mixed convection opposing flow correlations were experimentally validated.

Reference	Reynolds number	Grashof number	Prandtl number
Churchill [14]	$6.105\times10^3 < \mathrm{Re}_f < 6.6835\times10^4$	$18.89\times10^6 < \mathrm{Gr}_f < 22.52\times10^6$	$1.75 < \mathrm{Pr}_f < 2.09$
Jackson and Fewster [13]	$0.1\times10^4 < \mathrm{Re}_b < 4.0\times10^4$	$\overline{\mathrm{Gr}} < 3.0\times10^8$	$2.5 < \mathrm{Pr}_b < 7.0$
Aicher and Martin [1]	$3.0\times10^3 < \mathrm{Re}_b < 1.2\times10^5$	$3\times10^7 < \mathrm{Ra}_f < 1\times10^9$	$0.7 < \mathrm{Pr}_b < 5.0$
Swanson and Catton [11]	$6.0\times10^3 < \mathrm{Re}_b < 2.0\times10^4$	$1.0\times10^8 < \mathrm{Gr}_b < 2.0\times10^9$	$\mathrm{Pr}_b = 6.5$
Swanson and Catton [15]	$2.3\times10^3 < \mathrm{Re}_b < 2.0\times10^4$	$1.0\times10^6 < \mathrm{Gr}_b < 2.0\times10^9$	$0.7 < \mathrm{Pr}_b < 7.0$
P. Poskas and R. Poskas [16]	$0.4\times10^4 < \mathrm{Re}_b < 4\times10^4$	$1.7\times10^8 < \mathrm{Gr}_q < 1.4\times10^{10}$	$\mathrm{Pr}_b = 0.71$

parameters. Because Eq. (9) was originally used to predict heat transfer coefficients for a vertical plate, the distance from the channel inlet is used as the characteristic length; however, Churchill used the pipe diameter as the characteristic length instead. This choice of characteristic length is also found in the thermal–hydraulic system code (Section 2.3). The characteristic length is canceled out by expanding the dimensionless numbers on both sides of Eq. (9), indicating that the heat transfer coefficient does not depend on the choice of the characteristic length. Furthermore, a turbulent natural convection heat transfer correlation for a vertical plate can effectively predict heat transfer coefficients for a circular tube, except for low-Pr fluid and small tube diameter conditions that exhibit boundary layer merger (or boundary layer interference) [21–23]. As an example, Ohk and Chung [23] conducted numerical simulations for natural-convection heat transfer in circular tubes for $0.7 \le \mathrm{Pr} \le 2014$. They observed that the thermal boundary layer interference does not occur in pipes more than 3 cm in diameter, and Nu for tubes is approximately the same as that for vertical plates. Furthermore, it has been experimentally confirmed that Eq. (9) can be used to calculate the heat transfer coefficient regardless of channel geometries [21]. The experimentally validated range of parameters for Eq. (7) is listed in Table 2.

2.1.2. Jackson and Fewster. Jackson and Fewster [13] proposed a dependent parameter based on the model developed by Hall and Jackson [24] and a semianalytical correlation whose model constants were determined based on experiments they conducted for mixed convection in a vertical tube. For a fully developed turbulence, integrated buoyant forces acting on a thermal boundary layer with a thickness of δ_T equals the shear stress difference, i.e., an increase from the wall shear stress (Appendix A).

$$\Delta\tau = \int_0^{\delta_T} (\rho_b - \rho) g dy \approx (\rho_b - \bar{\rho}) g \delta_T, \tag{10}$$

where y is the distance from the heated wall. The nondimensional equations of Eq. (10) are Eq. (11a) for forced convection and Eq. (11b) for natural convection (Appendix B).

$$\frac{\Delta\tau}{\tau_w} \approx K_1 \frac{\bar{\mathrm{Gr}}}{\mathrm{Re}_b^{2.625}\,\mathrm{Pr}_b^{0.5}}, \tag{11a}$$

$$\frac{\Delta\tau}{\tau_w} \approx K_2 \left(\frac{\bar{\mathrm{Gr}}}{\mathrm{Re}_b^{2.625}\mathrm{Pr}_b^{0.5}}\right)^{2/3}, \tag{11b}$$

where K_1 and K_2 are the proportionality factors and τ_w is the wall shear stress. Equations (11a) and (11b) indicate that parameter $\overline{\mathrm{Gr}}/(\mathrm{Re}_b^{2.625}\mathrm{Pr}_b^{0.5})$ is a fundamental parameter for the shear stress difference $\Delta\tau/\tau_w$ for forced and natural convection. $\overline{\mathrm{Gr}}$ is the Gr with a different definition from the Gr in Eq. (1b) and is defined by Eq. (5). The characteristic length is the tube diameter. Jackson and Fewster assumed that the increase in the shear stress due to buoyancy $\Delta\tau/\tau_w$ is similar to the increase in the heat transfer coefficient $\mathrm{Nu}_b/\mathrm{Nu}_{0,b}$ based on the heat and momentum transport analogy and modeled $\mathrm{Nu}_b/\mathrm{Nu}_{0,b}$ as

$$\frac{\mathrm{Nu}_b}{\mathrm{Nu}_{0,b}} = \phi\left(\frac{\overline{\mathrm{Gr}}}{\mathrm{Re}_b^{2.625}\mathrm{Pr}_b^{0.5}}\right), \tag{12}$$

where $\mathrm{Nu}_{0,b}$ is the Nu for the forced convection. The increase in the shear stress due to buoyancy in mixed convection is regarded as the increase in the shear stress in forced convection. In other words, the shear stress of mixed convection is that of the forced convection with the enhanced Re by the buoyancy effect: $\mathrm{Re}_b' > \mathrm{Re}_b$. Variables with ($'$) are the forced convection for Re'. Assuming that Nu_0 and the friction coefficient $c_f = \tau_w/(0.5\rho_b v_m^2)$ for forced convection are proportional to $\mathrm{Re}_b^{0.82}$ and $\mathrm{Re}_b^{-0.25}$, respectively, Eq. (13) is obtained. This assumption affects the dependent parameter and the exponent 0.47 in the following equation (Appendix C):

$$\frac{h'}{h} = \left(\frac{\tau_w + \Delta\tau}{\tau_w}\right)^{0.47}. \tag{13}$$

Using Eq. (11a), Jackson and Fewster finally obtain

$$\frac{\mathrm{Nu}_b}{\mathrm{Nu}_{0,b}} = \left(1 + K_1 \frac{\overline{\mathrm{Gr}}}{\mathrm{Re}_b^{2.625}\mathrm{Pr}_b^{0.5}}\right)^{0.47}. \tag{14}$$

Nu_b for natural convection should not depend on Re_b. However, when Eq. (14) is applied to conditions where natural convection prevails ($1 \ll K_1\overline{\mathrm{Gr}}/\mathrm{Re}_b^{2.625}\mathrm{Pr}_b^{0.5}$), Nu_b slightly depends on Re_b. To eliminate the Nu_b dependency on Re_b, Jackson and Fewster modified the exponent from 0.47 to 0.31. Jackson and Fewster conducted mixed convection experiments to determine K_1 and obtained Eq. (15). The experimental apparatus is a circular tube with an inner diameter of 98.4 mm and a length of 9 m. The thermal boundary condition at the wall is the uniform heat flux (UHF) condition.

$$\frac{\mathrm{Nu}_b}{\mathrm{Nu}_{0,b}} = \left(1 + 4500 \frac{\overline{\mathrm{Gr}}}{\mathrm{Re}_b^{2.625}\mathrm{Pr}_b^{0.5}}\right)^{0.31}. \tag{15}$$

Physical properties are evaluated at the fluid bulk temperature, except for density, because, according to Jackson and Fewster, the experimental data correlate better with the bulk temperature than the film temperature. $\mathrm{Nu}_{0,b}$ is calculated using the Petukhov and Kirrilov correlation [25], multiplied by 1.16.

$$\mathrm{Nu}_{0,b} = \frac{\mathrm{Re}_b\,\mathrm{Pr}_b\,(c_f/2)}{12.7(c_f/2)^{1/2}\left(\mathrm{Pr}_b^{2/3} - 1\right) + 1.07}, \tag{16a}$$

$$c_f = \frac{1}{(3.64\log\ \mathrm{Re}_b - 3.28)^2}. \tag{16b}$$

Jackson and Fewster multiplied Eq. (16a) by 1.16 to reproduce their experimental value because a systematic discrepancy exists between the experimental results for high Re_b

and Eqs. (16a) and (16b). Table 2 shows the experimental parameter ranges. Equation (17) gives the dependent parameter range over which Eq. (15) is validated experimentally. As shown in Section 4.3, the mixed convection heat transfer correlation Eq. (15) is excellent in extrapolation performance to forced and natural convection-dominant conditions.

$$10^{-5} < \frac{\overline{\mathrm{Gr}}}{\mathrm{Re}_b^{2.625}\mathrm{Pr}_b^{0.5}} < 0.2. \tag{17}$$

The difference in the thermal boundary conditions between UWT and UHF has no significant effect on Nu for mixed convection if the flow is turbulent, similar to forced and natural convection [17, 19]. It is experimentally confirmed that the Jackson and Fewster correlation applies to UWT experiments [26]. The critical Re, where the differences in the thermal boundary condition lose influence on heat transfer, depends on Gr_b. According to Joye [27], when Re_b is larger than that given by the following equation, the difference in the thermal boundary conditions no longer affects heat transfer.

$$\mathrm{Re}_b = \frac{0.36\left\{\mathrm{Gr}_b(L/D)^3\right\}^{1/3}}{\mathrm{Pr}_b^{2/3}}. \tag{18}$$

2.1.3. Aicher and Martin. Aicher and Martin [1] proposed the interpolation formula using a forced and natural convection heat transfer correlation based on the same idea as the Churchill correlation Eq. (7) and determined its exponent from their experimental data. The experimental apparatus is a double-pipe heat exchanger. The test section is the inner circular tube, and water flows through the outer annular section at high velocity to impose the UWT thermal boundary condition. The inner diameter D and the length L of the inner tube constituting the test section are $(D, L) = (27, 2000)$, $(D, L) = (37, 2000)$, and $(D, L) = (37, 920)$ mm. The working fluid is water. The physical properties comprising the Re were evaluated at the mean bulk temperature, defined as the arithmetic mean of the inlet and outlet temperatures. The physical properties comprising the Ra were evaluated at the film temperature, defined as the arithmetic mean of the mean bulk and wall temperatures. The proposed correlation for the opposing mixed convection is

$$\bar{\mathrm{Nu}}_b = \sqrt{\mathrm{Nu}_{\mathrm{ft},b}^2 + \mathrm{Nu}_{\mathrm{nt},b}^2}. \tag{19}$$

The Gnielinski correlation [28], which is applicable from transition to turbulent flow, is adopted for a forced convection heat transfer correlation $\mathrm{Nu}_{\mathrm{ft},b}$. The Gnielinski correlation uses the following equation for a fully developed turbulent flow $\mathrm{Re}_b \geq 1.0 \times 10^4$:

$$\mathrm{Nu}_{\mathrm{ft},b} = \frac{(f/8)\ \mathrm{Re}_b\,\mathrm{Pr}_b}{1 + 12.7\sqrt{f/8}\left(\mathrm{Pr}_b^{2/3} - 1\right)}\left\{1 + \left(\frac{D}{L}\right)^{2/3}\right\}, \tag{20a}$$

$$f = (1.8\log\ \mathrm{Re}_b - 1.5)^{-2}. \tag{20b}$$

Equations (20a) and (20b) originally include a factor to correct the temperature dependency of the physical property $(\mathrm{Pr}_b/\mathrm{Pr}_w)^{0.11}$, but Aicher and Martine removed it [1]. The factor can be ignored under conditions where the temperature difference is not substantial because it corrects the effect of spatial temperature nonuniformity. The transition regime $2.3 \times 10^3 < \mathrm{Re}_b < 1.0 \times 10^4$ is interpolated as

$$\mathrm{Nu}_{\mathrm{ft},b} = (1-\gamma)\mathrm{Nu}_{\mathrm{fl},b}\big|_{\mathrm{Re}_b=2300} + \gamma\mathrm{Nu}_{\mathrm{ft},b}\big|_{\mathrm{Re}_b=10000}, \tag{21a}$$

$$\gamma = \frac{\mathrm{Re}_b - 2300}{10000 - 2300}, \tag{21b}$$

where $\mathrm{Nu}_{\mathrm{fl},b}$ is given as follows using the Graetz number $(\mathrm{Gz}_b = \mathrm{Re}_b\,\mathrm{Pr}_b\,D/L)$ [29]:

$$\mathrm{Nu}_{\mathrm{fl},b} = \left[3.66^3 + 0.7^3 + \left(1.615\mathrm{Gz}_b^{2/3} - 0.7\right)^3 + \left\{\left(\frac{2}{1+22\mathrm{Pr}_b}\right)^{1/6}\sqrt{\mathrm{Gz}_b}\right\}^3\right]^{1/3}. \tag{22}$$

The modified Churchill and Chu [19] correlation, whose model constant was re-evaluated by Aicher and Martin based on the experimental data [20, 30–34] in a pipe extracted from the mixed convection experiments conducted under the natural convection dominant condition ($\mathrm{Ra}_f^{0.333}/\mathrm{Re}_b^{0.8}\,\mathrm{Pr}_b^{0.4} > 0.2$), is adopted for the turbulent natural convection correlation $\mathrm{Nu}_{\mathrm{nt},b}$.

$$\mathrm{Nu}_{\mathrm{nt},b} = 0.122\,\mathrm{Ra}_f^{0.333}\left\{1 + \left(\frac{0.492}{\mathrm{Pr}_b}\right)^{9/16}\right\}^{-16/27}. \tag{23}$$

2.2. Vertical Rectangular Duct

2.2.1. Swanson and Catton (JHT). In this study, the authors term the short-side length of a rectangular channel cross-section as the gap and the long-side length as the channel width. Swanson and Catton [11] conducted mixed convection opposing flow experiments, wherein both sides of a rectangular duct with 108 cm × 4.445 cm × 43.2 cm (length × gap × width) were heated under the UHF condition using film-type heaters and proposed the following correlation. Figure 2(b) shows the schematic diagram of the test section. The working fluid used was Freon-113. The characteristic length and dependent parameter were the hydraulic-equivalent diameter and $\mathrm{Gr}/\mathrm{Re}^2$, respectively.

$$\frac{\bar{\mathrm{Nu}}}{\mathrm{Nu}_0} = 1.0 + 0.9\left\{\ln\left(\frac{\mathrm{Gr}}{\mathrm{Re}^2} + 1\right)\right\}^{1.39}. \tag{24}$$

The Petukhov and Kirillov correlation (Eqs. (16a) and (16b)) is used to calculate Nu_0. The physical properties of the fluid were evaluated at the average duct temperature [35]. This equation does not indicate the dependence of Nu on Pr and has not been validated for any other fluid except Freon-113 by Swanson and Catton. Equation (24) is verified experimentally for the parameter ranges listed in

Table 2. The dependent parameter range, for which the correlation has been validated experimentally, is

$$0.9 < \frac{\mathrm{Gr}}{\mathrm{Re}^2} < 30. \tag{25}$$

Equation (24) has been implemented in the system codes, including RELAP5 and TRACE, as the heat transfer correlation for single-phase mixed convection flows (Section 2.3).

2.2.2. Swanson and Catton (IJHMT). Swanson and Catton [15] applied the surface renewal theory to mixed convection opposing flow to derive an analytical expression of a heat transfer coefficient. They proposed a semianalytical equation whose constants were modified based on the results of their rectangular duct experiments using Freon-113 (Section 2.2.1) as a working fluid. Figure 2(b) shows the schematic diagram of the test section. The UHF is the thermal boundary condition on the wall. The surface renewal theory proposed by Danckwerts [36] was originally developed for a gas absorption problem to the liquid phase at a gas–liquid interface, and Hanratty [37] and Thomas et al. [38–40] improved and applied it to wall turbulence. The surface renewal theory assumes that heat exchange occurs by intermittently replacing fluid clumps in the viscous sublayer near the heated wall with bulk fluid (renewal of the surface). The theory assumes that the fluid clumps next to the wall have an age, or a residence time, distribution at an arbitrary time, with a variable $\psi = (v, P, T)$ representing physical variables, such as the velocity v, the pressure P, and the temperature T, and the time average $\bar{\psi}$ was defined as

$$\bar{\psi} = \int_0^\infty \psi(t, y)\phi(t)dt, \tag{26}$$

where y is the distance from the wall, t is the time, and $\phi(t)$ is the distribution function indicating the time since a fluid clump is exposed to the wall. Danckwerts' random contact time distribution is frequently used.

$$\phi(t) = \frac{1}{\tau}e^{-t/\tau}, \tag{27}$$

where τ is the nondimensional mean wall residence time. Constant physical properties, incompressible flow, fully developed turbulence, boundary layer approximation, Boussinesq's approximation, and negligible effects of stream-wise convective heat transport were assumed. By multiplying the momentum and energy transport equations holding near the heated wall by $\phi(t)$ and integrating them from 0 to ∞, Swanson and Catton obtained

$$\frac{1}{\tau}(\bar{v} - \bar{v}_i) = -\frac{\partial \bar{P}}{\partial x} - \frac{\mathrm{Gr}}{\mathrm{Re}^2}\bar{T} + \frac{1}{\mathrm{Re}}\frac{\partial^2 \bar{v}}{\partial y^2}, \tag{28a}$$

$$\frac{1}{\tau}\left(\bar{T} - \bar{T}_i\right) = \frac{1}{\mathrm{Pe}}\frac{\partial^2 \bar{T}}{\partial y^2}, \tag{28b}$$

where v_i and T_i are the initial velocity and temperature, respectively. The fluid physical properties were evaluated at the average duct temperature [35]. Pe($\equiv$Re Pr) is the Péclet number. The governing equation (Eqs. (28a) and (28b)) can be solved under the appropriate boundary conditions, and finally, Swanson and Catton obtained

$$\mathrm{Nu} = 0.0115\,\mathrm{Re}^{0.8}\,\mathrm{Pr}^{0.5}\left[1 + \left\{1 - \frac{696}{\mathrm{Re}^{0.8}} + 7561\frac{\mathrm{Gr}}{\mathrm{Re}^{2.6}\,(\mathrm{Pr}^{0.5} + 1)}\right\}^{0.5}\right]. \tag{29}$$

Swanson and Catton proposed the following semianalytical equation by modifying the constant and the exponent included in the above equation based on their experimental data.

$$\mathrm{Nu} = 0.0115\,\mathrm{Re}^{0.8}\,\mathrm{Pr}^{0.5}\left[1 + \left\{1 - \frac{696}{\mathrm{Re}^{0.8}} + 8300\frac{\mathrm{Gr}}{\mathrm{Re}^{2.6}\,(\mathrm{Pr}^{0.5} + 1)}\right\}^{0.39}\right]. \tag{30}$$

The buoyancy term can be ignored for forced convection.

$$\mathrm{Nu}_0 = 0.0115\,\mathrm{Re}^{0.8}\,\mathrm{Pr}^{0.5}\left\{1 + \left(1 - \frac{696}{\mathrm{Re}^{0.8}}\right)^{0.39}\right\}. \tag{31}$$

The term $696/\mathrm{Re}^{0.8}$ can be neglected for Re > 10000, and the above equation asymptotically approaches the Dittus and Boelter equation (described later, Eq. (45)). By normalizing Eq. (30) using Eq. (31), the following equation is given:

$$\frac{\mathrm{Nu}}{\mathrm{Nu}_0} = \frac{1 + \left\{1 - \left(696/\mathrm{Re}^{0.8}\right) + 8300\left(\mathrm{Gr}/\mathrm{Re}^{2.6}\left(\mathrm{Pr}^{0.5} + 1\right)\right)\right\}^{0.39}}{1 + \left(1 - \left(696/\mathrm{Re}^{0.8}\right)\right)^{0.39}}. \tag{32}$$

Table 2 shows the range where the validity of the equation has been experimentally confirmed. Since Swanson and Catton proposed two different correlations in different journals in the same year, Eqs. (24) and (30) are denoted Swanson and Catton (JHT) and Swanson and Catton (IJHMT), respectively, to distinguish the two correlations.

2.2.3. P. Poskas and R. Poskas. P. Poskas and R. Poskas [16] proposed an empirical correlation based on the experimental results in a rectangular duct whose only one side was heated under the UHF condition. The experimental apparatus was a rectangular duct with 6260 × 40.8 × 400 mm (length × gap × width), and the working fluid was air. Figure 2(c) shows the schematic diagram of the test section.

$$\frac{\mathrm{Nu}_b}{\mathrm{Nu}_{0,b}} = 1 + 1.65\left(\frac{\mathrm{Gr}_q}{\mathrm{Re}_b^{2.5}\,\mathrm{Pr}_b^{0.8}}\right)^{0.8}. \tag{33}$$

The hydraulic-equivalent diameter, the fluid bulk temperature, and the bulk velocity were used as the characteristic scales comprising the nondimensional numbers. The Grashof number Gr_q was defined as Eq. (4). Table 2 shows the parameter ranges over which the experiments were

performed. The assumption of constant physical properties is reasonable when the temperature difference is small. However, when the temperature difference is considerable, correlations considering the physical properties of nonuniformity provide a more accurate prediction. For the forced convection heat transfer correlation $\mathrm{Nu}_{0,b}$, P. Poskas and R. Poskas used the correlation proposed by Vilemas et al. [41] for an annular duct to include the effect of the temperature dependence of the physical property on heat transfer.

$$\frac{\mathrm{Nu}_{0,b}}{\mathrm{Nu}_{\mathrm{cp}}} = 1 - 0.744\left[1 - \exp\left\{-K_f\left(0.26F + 0.7\Phi K_f\right)\right\}\right], \tag{34a}$$

$$F = 1 - \exp\left(-0.1\tilde{x}\right), \tag{34b}$$

$$\Phi = \frac{1.25\left(0.01\tilde{x}\right)^2}{1 + \left(0.01\tilde{x}\right)^2}, \tag{34c}$$

$$\tilde{x} = \frac{x}{D_h}, \tag{34d}$$

$$K_f = \frac{q_w'' D_h}{k\, T\, \mathrm{Nu}_{\psi=1}}, \tag{34e}$$

where x is the distance from the duct inlet. $\mathrm{Nu}_{\mathrm{cp}}$ is the Nusselt number for when the physical properties are constant, and the following correlation is used:

$$\mathrm{Nu}_{\mathrm{cp}} = 0.01935\ \mathrm{Re}_b^{0.8}\,\mathrm{Pr}_b^{0.6}\left(0.86 + 0.8\tilde{x}^{-0.4}\right). \tag{35}$$

A relationship $\mathrm{Nu}|_{\mathrm{anular}}/\mathrm{Nu}|_{\mathrm{tube}} = 0.86\left(d_i/d_o\right)^{-0.16}$ [42] exists for turbulent forced convection, where $\mathrm{Nu}|_{\mathrm{anular}}$ is for an annular duct with a heated inner wall and an adiabatic outer wall and $\mathrm{Nu}|_{\mathrm{tube}}$ is for a circular tube. d_i and d_o are the inner and outer diameters, respectively. The characteristic length is the hydraulic-equivalent diameter: $D_h = d_o - d_i$. According to this relationship, the ratio of the Nusselt number for a one-side heating parallel plate and circular tube could be $\mathrm{Nu}|_{\mathrm{plates}} \approx 0.86\,\mathrm{Nu}|_{\mathrm{tube}}$ because the curvature of the parallel plate was zero, resulting in $d_i/d_o \approx 1$.

2.3. Implementation of Single-Phase Flow Heat Transfer Correlations in Thermal–Hydraulic System Codes. A thermal–hydraulic reactor system code predicts an overall system behavior for a given event and provides boundary conditions for a stress analysis of the RPV wall in a downcomer. This section reviews the single-phase heat transfer correlations implemented in the typical thermal–hydraulic codes TRACE, RELAP5, and TRAC-PF1.

2.3.1. TRACE. The authors review the wall heat transfer correlations implemented in TRACE V5.0/P6 [4], the latest version. The TRACE code uses different heat transfer correlations depending on a selected channel geometry. The heat transfer correlations for tube or rectangular duct geometry are applied for downcomers. TRACE uses the hydraulic-equivalent diameter D_h as the characteristic length. The density in the Grashof number is evaluated at the film temperature, and the other physical properties are evaluated at the fluid bulk temperature.

(1) Tube Geometry. When the tube geometry is selected, the heat transfer correlations for a laminar forced convection h_{fl}, a turbulent forced convection h_{ft}, a laminar natural convection h_{nl}, and a turbulent natural h_{nt} convection are evaluated, and the largest one is adopted. A mixed convection heat transfer correlation is not implemented in this geometry. Each heat transfer coefficient is calculated from the Nu correlation. The laminar forced convection $\mathrm{Nu}_{\mathrm{fl}}$ is calculated using an analytical solution [43] for a fully developed laminar flow in a circular tube heated with the UHF condition.

$$\mathrm{Nu}_{\mathrm{fl},b} = 4.36. \tag{36}$$

The turbulent forced convection $\mathrm{Nu}_{\mathrm{ft}}$ is calculated using the Gnielinski correlation [44].

$$\mathrm{Nu}_{\mathrm{ft},b} = \frac{\left(c_f/2\right)\left(\mathrm{Re}_b - 1000\right)\mathrm{Pr}_b}{1 + 12.7\sqrt{c_f/2}\left(\mathrm{Pr}_b^{2/3} - 1\right)}, \tag{37a}$$

$$c_f = \left(1.58\ln\ \mathrm{Re}_b - 3.28\right)^{-2}. \tag{37b}$$

The range of applicability of this correlation is as follows:

$$2.3 \times 10^3 \le \mathrm{Re}_b \le 5 \times 10^6, \tag{38a}$$

$$0.5 \le \mathrm{Pr}_b \le 2.0 \times 10^3. \tag{38b}$$

When the temperature difference is meaningful, the correlation considering the physical property nonuniformity improves the prediction. The TRACE uses Hufschmidt and Burck's equation [45] to correct the effect of the physical property variation.

$$\mathrm{Nu}_{\mathrm{ft},b} = \mathrm{Nu}_{\mathrm{cp}}\left(\frac{\mathrm{Pr}_b}{\mathrm{Pr}_w}\right)^{0.11} \text{for } 0.05 \le \frac{\mathrm{Pr}_b}{\mathrm{Pr}_w} \le 20, \tag{39}$$

where the Nusselt number for uniform physical properties $\mathrm{Nu}_{\mathrm{cp}}$ is calculated using Eqs. (37a) and (37b). This correction is used for heated walls: $T_w > T_b$. The laminar $\mathrm{Nu}_{\mathrm{nl},b}$ and turbulent $\mathrm{Nu}_{\mathrm{nt},b}$ natural-convection heat transfer correlations are given by that for a vertical plate.

$$\mathrm{Nu}_{\mathrm{nl},b} = 0.59\left(\mathrm{Gr}_f\,\mathrm{Pr}_b\right)^{1/4}, \tag{40a}$$

$$\mathrm{Nu}_{\mathrm{nt},b} = 0.13\left(\mathrm{Gr}_f\,\mathrm{Pr}_b\right)^{1/3}, \tag{40b}$$

where Gr_f is the Grashof number, whose density is evaluated at the film temperature, and the other physical properties are evaluated at the bulk temperature. Correlations for a vertical plate use the plate height as the characteristic length, but TRACE uses the hydraulic-equivalent diameter instead. This characteristic length treatment is possible because the authors can show that the heat transfer correlation does not depend on the choice of the characteristic length by

expanding the nondimensional numbers in Eq. (40b) (Section 2.1.1).

(2) Rectangular Duct. A turbulent mixed convection heat transfer correlation h_{mt} is implemented in the rectangular duct geometry. Similar to the tube geometry, the heat transfer coefficient is calculated for each flow regime, including laminar forced convection, turbulent forced convection, laminar natural convection, and turbulent mixed convection, and then, the largest one is adopted.

$$h = \max\left(h_{\mathrm{fl}}, h_{\mathrm{ft}}, h_{\mathrm{nl}}, h_{\mathrm{mt}}\right). \tag{41}$$

The laminar natural-convection heat transfer correlation $\mathrm{Nu}_{\mathrm{nl},b}$ is calculated using the Elenbaas equation [46, 47].

$$\mathrm{Nu}_{\mathrm{nl},b} = \frac{R_h\,\mathrm{Ra}_{L,f}}{24L}\left[1 - \exp\left\{-24\left(\frac{L}{2\,R_h\,\mathrm{Ra}_{L,f}}\right)^{3/4}\right\}\right], \tag{42}$$

where R_h is the gap of a rectangular duct. The characteristic lengths for $\mathrm{Nu}_{\mathrm{nl},b}$ and $\mathrm{Ra}_{L,f}$ are R_h and L, respectively. TRACE uses Eq. (42) after converting it to the Nusselt number based on the hydraulic-equivalent diameter D_h: $\mathrm{Nu}_{\mathrm{nl},b}$ D_h/R_h. For the rectangular duct with a large aspect ratio, $D_h/R_h \approx 2$, the constants in Eq. (42) were determined for air, and the range validated by Elenbaas is

$$10^{-1} \le \frac{R_h}{L}\,\mathrm{Ra}_{R_h,f} \le 10^5, \tag{43}$$

where Ra_{R_h} is the Rayleigh number with R_h as the characteristic length. The heat transfer coefficient for laminar forced convection $\mathrm{Nu}_{\mathrm{fl},b}$ is calculated using the analytical equation for a rectangular duct heated with the UHF condition. The analytical equation is a function of the duct aspect ratio, but the value 7.63, calculated for an advanced neutron source (ANS) in the Oak Ridge National Laboratory (ORNL), has been implemented [48].

$$\mathrm{Nu}_{\mathrm{fl},b} = 7.63. \tag{44}$$

The Nusselt number for turbulent forced convection $\mathrm{Nu}_{\mathrm{ft},b}$ is calculated using the Petukhov and Kirillov correlation (Eqs. (16a) and (16b)). The Nusselt number for turbulent mixed convection $\mathrm{Nu}_{\mathrm{mt},b}$ is calculated by multiplying the Petukhov and Kirillov correlation (Eqs. (16a) and (16b)) by the Swannson and Catton correlation (Eq. (24)). The mixed convection correlation is applied only for $0.1 < \mathrm{Gr}_b/\mathrm{Re}_b^2$ and $\mathrm{Re}_b > 3000$.

2.3.2. RELAP5. Like the TRACE code, the RELAP5/MOD3.3 [2] also adopts different single-phase heat transfer correlations, depending on a selected channel geometry. The authors focus on the default and parallel plate geometries applied for heat transfer analysis in a downcomer. The characteristic length is the hydraulic-equivalent diameter, and the physical properties are evaluated at the fluid bulk temperature unless otherwise noted.

(1) Default Geometry. The heat transfer correlation for the default geometry is based on that in the fully developed pipe flow. As with the TRACE code, the largest Nusselt number for turbulent forced convection $\mathrm{Nu}_{\mathrm{ft},b}$, laminar forced convection $\mathrm{Nu}_{\mathrm{fl},b}$, and natural convection from laminar to turbulence $\mathrm{Nu}_{\mathrm{n},b}$ is adopted. Any mixed convection correlation is not implemented. The Nusselt number for laminar forced convection $\mathrm{Nu}_{\mathrm{fl},b}$ is given by the analytical solution for the UHF condition, same as TRACE (Eq. (36)). The Nusselt number for turbulent forced convection $\mathrm{Nu}_{\mathrm{ft},b}$ is given by the Dittus and Boelter equation.

$$\mathrm{Nu}_{\mathrm{ft},b} = 0.023\,\mathrm{Re}_b^{0.8}\,\mathrm{Pr}_b^n, \tag{45}$$

where $n = 0.4$ is used for the exponent of the Prandtl number. The Nusselt number correlation for natural convection $\mathrm{Nu}_{n,b}$ differs depending on whether the flow path is vertical or horizontal. For the vertical flow path like downcomers, the Churchill and Chu correlation [19], applicable to various conditions from laminar to turbulent flow, is adopted.

$$\mathrm{Nu}_{n,b} = \left[0.825 + \frac{0.387\mathrm{Ra}_b^{1/6}}{\left\{1 + \left(0.492/\mathrm{Pr}_b\right)^{9/16}\right\}^{8/27}}\right]^2. \tag{46}$$

(2) Parallel Plate Geometry. When the parallel plate geometry is selected, the Nusselt number for laminar forced convection $\mathrm{Nu}_{\mathrm{fl},b}$ is calculated using the analytical solution for the rectangular channel heated with the UHF condition (Eq. (44)). The Petukhov correlation [49] gives the Nusselt number for the turbulent forced convection $\mathrm{Nu}_{\mathrm{ft},b}$.

$$\mathrm{Nu}_{\mathrm{ft},b} = \frac{(f/8)\ \mathrm{Re}_b\,\mathrm{Pr}_b\left(\mu_b/\mu_w\right)^{0.11}}{1 + 3.4f + \left(11.7 + \left(1.8/\mathrm{Pr}_b^{1/3}\right)\right)\sqrt{f/8}\left(\mathrm{Pr}_b^{2/3} - 1\right)}, \tag{47a}$$

$$f = \frac{1.0875 - 0.1125\left(R_h/S\right)}{\left(1.82\ \log_{10}\mathrm{Re}_b - 1.64\right)^2}, \tag{47b}$$

where S is the width of the rectangular channel. The Nusselt number for laminar natural convection $\mathrm{Nu}_{\mathrm{nl},b}$ is given using the Elenbaas equation (Eq. (42)), same as TRACE. The parallel plate geometry considers turbulent mixed convection. The Nusselt number for mixed convection $\mathrm{Nu}_{\mathrm{mt},b}$ is calculated by multiplying the Nusselt number for the turbulent forced convection calculated by the Petukhov correlation Eqs. (47a) and (47b) with the Swanson and Catton correlation (Eq. (24)).

2.3.3. TRAC. The TRAC code has several variations. In this section, the authors review the wall heat transfer models implemented in the TRAC-PF1/MOD1 [9], a code with respect to PWR, because PWR is the primary objective of PTS analysis. TRAC-PF1/MOD1 selects a heat transfer

correlation from a generalized boiling curve. The flow regime is determined based on a logic chart. If the flow regime is judged as single-phase flow, the flow is considered to be forced convection for $\mathrm{Gr}_b/\mathrm{Re}_b^2 \leq 1$ and as natural convection for $\mathrm{Gr}_b/\mathrm{Re}_b^2 > 1$. A mixed convection correlation is not implemented in TRAC-PF1/MOD1. To calculate the Nusselt number corresponding to forced convection, the larger of the two heat transfer coefficients with respect to laminar and turbulent forced convections is used. For the laminar forced convection, the following equation [50] is used.

$$\mathrm{Nu}_{\mathrm{fl},b} = 4.0. \tag{48}$$

The Dittus and Boelter correlation (Eq. (45)) is adopted in the case of turbulent forced convection $\mathrm{Nu}_{\mathrm{ft},b}$, wherein the exponent of the Prandtl number is $n = 0.4$. To calculate the Nusselt number corresponding to natural convection, the larger of the two heat transfer coefficients with respect to laminar and turbulent natural convections is used. Equation (40a) is adopted in the case of laminar natural convection $\mathrm{Nu}_{\mathrm{nl},b}$. Equation (40b) is adopted in the case of turbulent natural convection $\mathrm{Nu}_{\mathrm{nt},b}$, wherein the model constant is 0.1 instead of 0.13. The characteristic length is taken to be the hydraulic-equivalent diameter. All physical properties are evaluated at the fluid bulk temperature, except for ρ_f and β in the Grashof number, which are calculated using the Taylor expansion at T_b as follows [9].

$$\rho_f = \rho_b + \frac{\partial \rho_b}{\partial T}\left(T_f - T_b\right), \tag{49a}$$

$$\beta = -\frac{\partial \rho_b}{\partial T}\frac{1}{\rho_f}. \tag{49b}$$

3. Verification of Existing Correlations Using Experimental Data

The experimental data published in the previous articles were typically provided with respect to the nondimensional parameters and a dependent parameter constructed based on those nondimensional parameters. Because the details of experimental boundary conditions, including the fluid bulk and wall temperatures, are usually not provided, directly comparing the existing heat transfer correlations with the experimental data is not easy. Using the following steps, the authors evaluate the predictive performance of the correlations described in Sections 2.1 and 2.2 by comparing them with the experimental data obtained using various working fluids and channel geometries.

Step 1. Select a database from among the experiments based on which the correlations were developed. The Axcell and Hall experiment [34], conducted using air in a vertical circular tube, and the Takeishi et al. experiment [51], wherein one-sided and two-sided heating experiments were conducted in a vertical rectangular duct, are added to the database for comparison because of their importance.

Step 2. Determine the boundary-condition ranges for the selected database based on the nondimensional number ranges over which the experiments were conducted.

Step 3. Randomly sample virtual experimental conditions, i.e., the boundary conditions and the characteristic length, within the range defined in Step 2.

Step 4. Calculate the nondimensional numbers for the virtual experimental conditions sampled in Step 3 and $\mathrm{Nu}/\mathrm{Nu}_0$ for the existing correlations.

Step 5. Compare the values predicted in Step 4 with the experimental data by plotting them against the same dependent parameter as in the experiment.

The definition of the nondimensional numbers and the temperature used to evaluate the physical properties are the same as in the experiments. The characteristic length is the hydraulic-equivalent diameter. For the Churchill correlation (Eq. (7)), all physical properties are evaluated at the film temperature according to the Herbert and Sterns experiment [20]. If the experimental data are given in a table for each nondimensional number, the authors use Jackson and Fewster's dependent parameter to compare the experimental data and correlation predictions. The comparison results are shown in Section 3 and discussed in Section 4.1.

3.1. Vertical Tube Experiment

3.1.1. Herbert and Sterns' Experiment. Table 3 lists the parameter ranges determined based on the Herbert and Sterns experiment [20]. Pr_f ranged from 1.75 to 2.09; therefore, the film temperature T_f can be calculated using any randomly selected Pr_f value from this range. The temperature difference ΔT can be calculated based on the randomly selected Gr_f in the range shown in Table 3. The wall and fluid bulk temperatures can be calculated from T_f and ΔT. The characteristic velocity can be calculated based on the randomly selected Re_f value between 6.105×10^3 and 6.684×10^4. Figure 3 shows the calculation results. The horizontal axis $\mathrm{Gr}_f/(\mathrm{Re}_f^{2.625}\mathrm{Pr}_f^{0.5})$ comprises nondimensional numbers with the same exponent as that in Jackson and Fewster's dependent parameter.

3.1.2. Jackson and Fewster's Experiment. Table 4 lists the parameter ranges determined based on the Jackson and Fewster experiment [13]. The values of Pr_b ranged from 2.5 to 7; hence, the bulk temperature T_b can be determined using randomly selected Pr_b values from this range. The wall temperature T_w can be calculated based on randomly selected Gr_w value between 5×10^6 and 1×10^8, where $\mathrm{Gr}_w \equiv (\rho_b - \rho_w)\,\rho_b\, g\, D^3/\mu_b^2$ is the Grashof number with a definition that is different from the definitions provided in Eq. (1b). The values of Re_b ranged from 1×10^3 to 4×10^4; therefore, the characteristic velocity is calculated using from randomly selected Re_b values in this range. Figure 4 shows the calculation results.

3.1.3. Aicher and Martine's Experiment. Table 5 summarizes the parameter ranges decided based on the Aicher and Martin experiment [1]. According to the article, Pr_b was 3–5.

Table 3: The calculation conditions used to evaluate the correlations for the Herbert and Sterns experiments [20].

Working fluid	Water
Thermal boundary condition	UWT
Hydraulic-equivalent diameter D_h (cm)	2.23
Reynolds number Re_f	6.105×10^3–6.684×10^4
Grashof number Gr_f	18.89×10^6–22.52×10^6
Prandtl number Pr_f	1.75–2.09

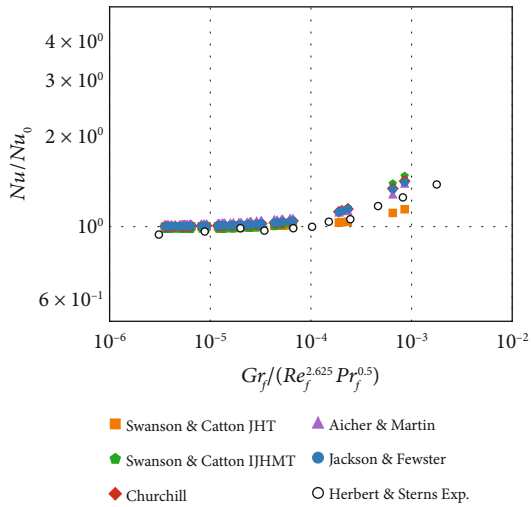

Figure 3: Enhancement factor $\mathrm{Nu}/\mathrm{Nu}_0$ predicted based on the Jackson and Fewster (Eq. (15)), Swanson and Catton JHT (Eq. (24)), Swanson and Catton IJHMT (Eq. (30)), Churchill (Eq. (7)), and Aicher and Martin (Eq. (19)) correlations. Experimental data are extracted from Herbert and Sterns experiments [20].

Table 4: The calculation conditions used to evaluate the correlations for the Jackson and Fewster experiments [13].

Working fluid	Water
Thermal boundary condition	UHF
Hydraulic-equivalent diameter D_h (cm)	9.84
Reynolds number Re_b	$1 \times 10^3 - 4 \times 10^4$
Grashof number Gr_w	$5 \times 10^6 - 1 \times 10^8$
Prandtl number Pr_b	2.5–7

The bulk temperatures T_b can be given from randomly selected Pr_b in the range. The experiments were performed for Re_b = 4,500, 7,500, 11,500, and 15,500. The characteristic velocity can be given by Re_b randomly selected from among those. The temperature differences can be obtained by randomly selected Ra_f from 10^6 to 10^9. Note that the physical properties are evaluated at the bulk temperature instead of the film temperature because it is unknown when evaluating ΔT from Ra_f. The authors conducted sensitivity analyses

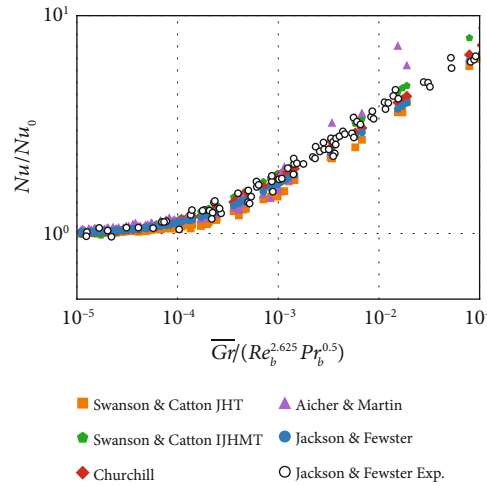

Figure 4: Enhancement factor $\mathrm{Nu}/\mathrm{Nu}_0$ predicted based on the Jackson and Fewster (Eq. (15)), Swanson and Catton JHT (Eq. (24)), Swanson and Catton IJHMT (Eq. (30)), Churchill (Eq. (7)), and Aicher and Martin (Eq. (19)) correlations. Experimental data are extracted from the Jackson and Fewster experiments [13].

Table 5: The calculation conditions used to evaluate the correlations for the Aicher and Martin experiments [1].

Working fluid	Water
Thermal boundary condition	UWT
Hydraulic-equivalent diameter D_h (cm)	2.7 and 3.7
Reynolds number Re_b	0.45×10^4, 0.75×10^4, 1.15×10^4, and 1.55×10^4
Rayleigh number Ra_f	10^6–10^9
Prandtl number Pr_b	3–5

and confirmed that this approximation does not significantly affect the calculation results. The calculation results are shown in Figure 5.

3.1.4. Axcell and Hall's Experiment. Axcell and Hall [34] conducted the mixed convection opposing flow experiments using air as the working fluid at atmospheric pressure in a vertical tube heated under the UWT condition. The experimental apparatus had a diameter of 0.613 m and a test-section length of 0.667 m. A preheated section of 4 m, with the same temperature as the test section, was located upstream from the test section. Table 6 lists the parameter ranges based on the Axcell and Hall experiment. The ranges with respect to the wall and bulk temperatures are extracted from the table shown in Axcell and Hall [34]. The difference between the wall and bulk temperatures is calculated based on the randomly selected values from these ranges. The characteristic velocity is calculated based on the Re_b value in the range extracted from the table shown in Axcell and Hall [34]. The integrated density is calculated using

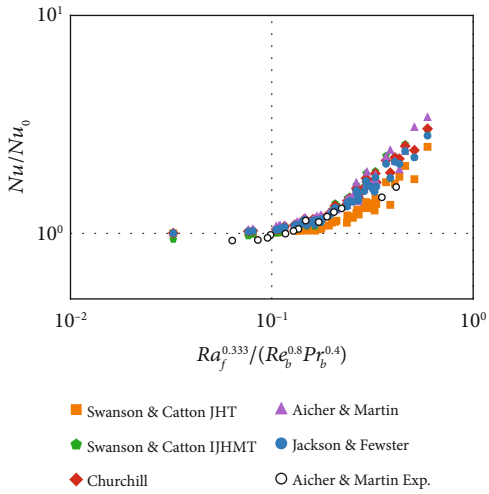

FIGURE 5: Enhancement factor Nu/Nu_0 predicted using the Jackson and Fewster (Eq. (15)), Swanson and Catton JHT (Eq. (24)), Swanson and Catton IJHMT (Eq. (30)), Churchill (Eq. (7)), and Aicher and Martin (Eq. (19)) correlations. Experimental data are extracted from the Aicher and Martin experiments [1].

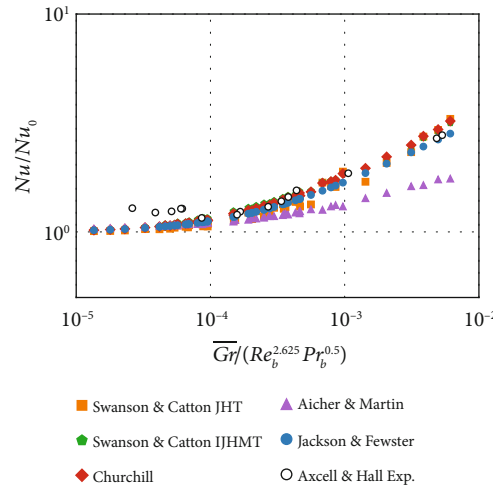

FIGURE 6: Enhancement factor Nu/Nu_0 predicted using the Jackson and Fewster (Eq. (15)), Swanson and Catton JHT (Eq. (24)), Swanson and Catton IJHMT (Eq. (30)), Churchill (Eq. (7)), and Aicher and Martin (Eq. (19)) correlations. Experimental data are extracted from the Axcell and Hall experiments [34].

TABLE 6: The calculation conditions used to evaluate the correlations with respect to the Axcell and Hall experiments [34].

Working fluid	Air
Thermal boundary condition	UWT
Pressure P (MPa)	0.1
Wall temperature T_w (K)	326.9–421.1
Bulk temperature T_b (K)	296.4–317.6
Hydraulic-equivalent diameter D_h (cm)	61.3
Reynolds number Re_b	0.179×10^5–1.261×10^5

TABLE 7: The calculation conditions used to evaluate the correlations with respect to the Swanson and Catton experiments [15, 35].

Working fluid	Freon-113
Thermal boundary condition	UHF
Hydraulic-equivalent diameter D_h (cm)	8.88
Reynolds number Re_b	$0.6 \times 10^4 - 2.0 \times 10^4$
Grashof number Gr_b	$0.1 \times 10^9 - 2.0 \times 10^9$
Prandtl number Pr_b	6.5

Eq. (6), and the other physical properties are evaluated using the bulk temperature. Figure 6 shows the calculation results.

3.2. Two-Side Wall Heating Experiments Using the Vertical Rectangular Duct

3.2.1. Swanson and Catton's Experiment. Table 7 lists the parameter ranges defined based on the Swanson and Catton experiment [15, 35]. The bulk temperature T_b was calculated using $Pr_b = 6.5$. The Re_b and Gr_b ranges are listed in Table 7 [35]. The characteristic velocity and temperature difference were calculated based on randomly selected Re_b and Gr_b values from these ranges, and Figure 7 shows the calculation results.

3.3. One-Side Wall Heating Experiments Using the Vertical Rectangular Duct

3.3.1. P. Poskas and R. Poskas' Experiment. Table 8 lists the parameter ranges based on the P. Poskas and R. Poskas experiment [16]. The working fluid used in the experiment was air, and one side of the rectangular duct was heated. P. Poskas and R. Poskas' experimental data were provided based on the Grashof number Gr_q defined using the wall heat flux q_w'', which is correlated to Gr_b, as shown in Eq. (4). Preliminary calculations confirmed that $\bar{Gr}/Gr_b \approx 0.45$ and $Gr_f/Gr_b \approx 0.7$ in the parameter range with respect to the P. Poskas and R. Poskas experiments. Sensitivity analysis confirmed that this approximation does not substantially affect the distribution of the predicted values. By substituting the approximation $Gr_q = Gr_b Nu_b \approx Gr_f Nu_b/0.7 \approx \bar{G}r Nu_b/0.45$ into each correlation, the authors can transform the correlations described based on Gr_b, Gr_f, and $\bar{G}r$ into those described based on Gr_q. After the random sampling of Re_b and Gr_q, Nu_b for each correlation can be calculated using the correlation expressed based on Gr_q via iterative calculations, and Figure 8 shows the calculation results.

3.3.2. Takeishi et al.'s Experiment. Takeishi et al. [51] conducted mixed convection opposing flow experiments using a vertical duct for one- and two-side heating under the UWT condition. The working fluid used in the experiments was air. The duct was 4 m in length and 0.6 m in width, and

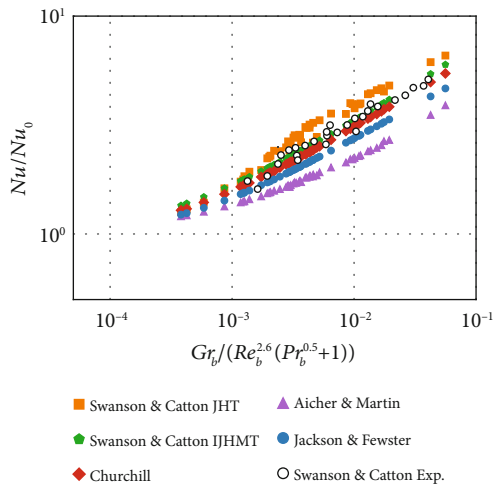

Figure 7: Enhancement factor Nu/Nu_0 predicted using the Jackson and Fewster (Eq. (15)), Swanson and Catton JHT (Eq. (24)), Swanson and Catton IJHMT (Eq. (30)), Churchill (Eq. (7)), and Aicher and Martin (Eq. (19)) correlations. Experimental data are extracted from the Swanson and Catton experiments [15].

Table 8: The calculation conditions used to evaluate the correlations with respect to the P. Poskas and R. Poskas experiments [16].

Working fluid	Air
Thermal boundary condition	UHF
Reynolds number Re_b	$4 \times 10^3 - 4 \times 10^4$
Grashof number Gr_q	$1.7 \times 10^8 - 1.4 \times 10^{10}$
Prandtl number Pr_b	0.7

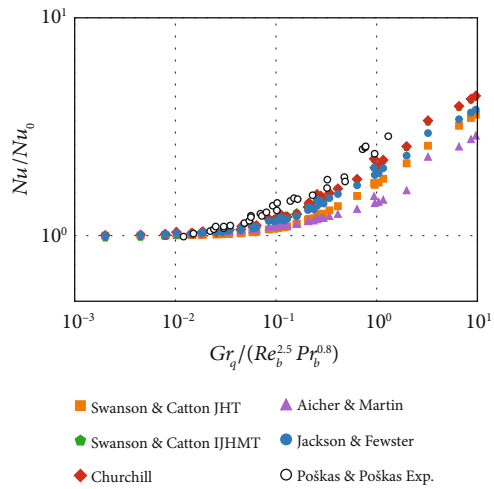

Figure 8: Enhancement factor Nu/Nu_0 predicted using the Jackson and Fewster (Eq. (15)), Swanson and Catton JHT (Eq. (24)), Swanson and Catton IJHMT (Eq. (30)), Churchill (Eq. (7)), and Aicher and Martin (Eq. (19)) correlations. Experimental data are extracted from the P. Poskas and R. Poskas experiments [16].

Table 9: The calculation conditions used to evaluate the correlations with respect to the Takeishi et al. experiments [51].

Working fluid	Air
Thermal boundary condition	UWT
Pressure P (MPa)	0.1
Wall temperature T_w (K)	303.15–373.15
Bulk temperature T_b (K)	293.15–363.15
Temperature difference $\Delta T = T_w - T_b$ (K)	10.0–70.0
Hydraulic-equivalent diameter D_h (cm)	20
Velocity v_g (m/s)	0–15.0

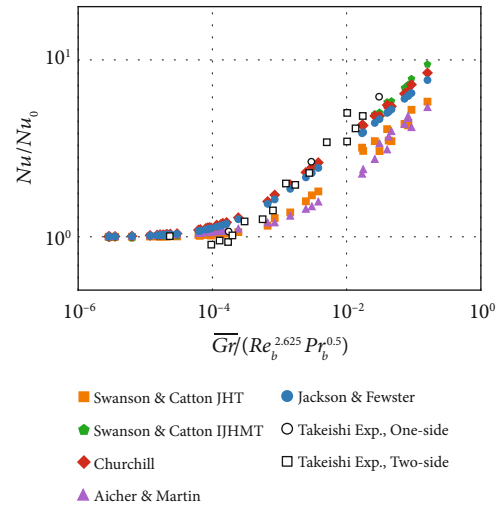

Figure 9: Enhancement factor Nu/Nu_0 predicted by the Jackson and Fewster (Eq. (15)), Swanson and Catton JHT (Eq. (24)), Swanson and Catton IJHMT (Eq. (30)), Churchill (Eq. (7)), and Aicher and Martin (Eq. (19)) correlations. Experimental data are extracted from the Takeishi et al. experiments [51].

its gap could be varied between 0 and 25 cm. The authors focus on the data obtained from the experiments using a gap of 10 cm. Table 9 lists the calculation conditions. The ranges of the pressure, the temperature difference, the hydraulic diameter D_h, and the velocity are obtained from Takeishi et al. [51]. The ranges of the temperature difference ΔT and the bulk temperature T_b were determined as the range listed in Table 9, with reference to the figures in Takeishi et al. [51]. The wall temperature T_w was calculated based on the randomly selected ΔT and T_b within the range listed in Table 9. The value of characteristic velocity is selected from the range of 0–15 m/s, and Figure 9 shows the calculation results. The experimental data for one- and two-side heating are shown in Figure 9.

4. Discussion

4.1. Accuracy of Correlations

4.1.1. Effect of the Thermal Boundary Condition. The correlations based on the data for the UHF experiments,

including the Jackson and Fewster (Eq. (15)) and the Swanson and Catton (Eqs. (24) and (30)) correlations, can effectively predict the data for the UWT experiments, including the Herbert and Sterns (Figure 3) and Axcell and Hall (Figure 6) experiments. Conversely, the correlations based on the data for the UWT experiments, including the Churchill (Eq. (7)) and the Aicher and Martin (Eq. (19)) correlations, can effectively predict the data for the UHF experiments, including the Jackson and Fewster experiment (Figure 4). The heat transfer correlations for turbulent mixed convection can be applied regardless of the thermal boundary conditions similar to the cases for turbulent forced and natural convection [17, 19].

4.1.2. Effect of Channel Geometry. The Jackson and Fewster correlation that is based on the experiment with respect to the flow of water in a vertical tube can reproduce the Swanson and Catton experiment (Figure 7), which is conducted with respect to the flow of Freon-113 in a vertical rectangular duct, and the Takeishi et al. experiment (Figure 9), which is conducted with respect to the flow of air in a vertical rectangular duct, using the hydraulic-equivalent diameter as the characteristic length. The Swanson and Catton correlation can reproduce the Axcell and Hall experiment (Figure 6), which is conducted with respect to the flow of air in a circular tube, using the hydraulic-equivalent diameter as the characteristic length. Therefore, the correlations can predict experiments regardless of the channel geometries using the hydraulic-equivalent diameter as a characteristic length. This is because $\mathrm{Nu}/\mathrm{Nu}_0$ is less sensitive to the characteristic length. For example, because the dependent parameter of the Jackson and Fewster correlation is $\bar{\mathrm{G}}\mathrm{r}/\mathrm{Re}_b^{2.625}\mathrm{Pr}_b^{0.5} \sim D_h^{0.375}$, even if D_h is doubled in the range where the validity has been confirmed experimentally, the effect of D_h on $\mathrm{Nu}/\mathrm{Nu}_0$ is less than 8.3%.

4.1.3. Effect of the Working Fluid. The correlations can predict experimental data regardless of the working fluid differences, indicating that the nondimensional numbers appearing in the correlations and their combinations are appropriate.

4.1.4. Effect of the Heating Wall. The Churchill (Eq. (7)), Jackson and Fewster, and Swanson and Catton (IJHMT) correlations (Eq. (30)) can effectively predict the one-side heating experiments performed by P. Poskas and R. Poskas (Figure 8) and Takeishi et al. (Figure 9), indicating that the existing mixed convection correlations can be used for predicting one- and two-side heating.

4.1.5. Prediction Accuracy. Although all the correlations can predict the experimental data effectively, the Jackson and Fewster, Churchill, and Swanson and Catton (IJHMT) correlations can predict the experimental data with high accuracy.

4.2. Comparison among Experimental Data. Each heat transfer correlation uses different definitions, even for a nondimensional number with a specific physical meaning, e.g., the Grashof number. To make the comparison among the experimental data easy, the authors study the relationships among the dependent parameters using the dependent parameter introduced in the Jackson and Fewster correlation, which has excellent predictivity as a representative parameter. Figure 10 shows the relationships between each dependent parameter adopted in each experiment (the vertical axes) and Jackson and Fewster's dependent parameter (the horizontal axes) for the sampling data provided in Section 3: (a) Herbert and Sterns [20], (b) Aicher and Martin [1], (c) Axcell and Hall [34], (d) Swanson and Catton (IJHMT) [15], (e) P. Poskas and R. Poskas [16], and (f) Takeshi et al. [51]. The figures show strong correlations between Jackson and Fewster's and other dependent parameters. These correlation relations (the solid lines in the figures) enable the conversion of a dependent parameter into another. Hence, the experimental data can be compared directly. The fitting curves are applied only within the range wherein the correlation relations are confirmed among the calculated dependent parameters.

Figure 11 compares the experimental data extracted from each study and converted into Jackson and Fewster's dependent parameter using the fitting curves that represent the relationships among the dependent parameters given in Figure 10. All experimental results are distributed along a single line, despite the differences in channel geometries, parameter ranges, and working fluids. The experimental data reasonably agree with the Jackson and Fewster correlation, the solid line in Figure 11, indicating that the experimental data for mixed convection opposing flow are effectively represented using the Jackson and Fewster's dependent parameter. This result is consistent with the fact that Jackson and Fewster's correlation could predict all experimental results in Section 3.

4.3. Extrapolation Performance under Forced and Natural Convection Conditions. Mixed convection heat transfer correlations are required to apply in a wide range from forced to natural convection-dominant conditions; i.e., they can be extrapolated to two dominant conditions. The extrapolation performance of the mixed convection heat transfer correlations can be evaluated by whether the correlation asymptotically approaches forced and natural convection heat transfer correlations under forced and natural convection-dominant conditions, respectively. Figure 12 shows the predictive performance of the mixed convection heat transfer correlation under forced (Figure 12(a)) and natural convection-dominant (Figure 12(b)) conditions. The authors sample the dimensionless numbers in a wider range of conditions than the range over which each correlation was experimentally validated by the correlation developers (Table 2) and calculate the predictions by each correlation. Since the definitions of the nondimensional numbers used in each correlation differ, the authors approximate them as $\mathrm{Pr} = \mathrm{Pr}_b \approx \mathrm{Pr}_f$, $\mathrm{Re} = \mathrm{Re}_b \approx \mathrm{Re}_f$, and $\mathrm{Gr} = \mathrm{Gr}_b \approx \mathrm{Gr}_f \approx 2\bar{\mathrm{G}}\mathrm{r}$. This approximation is more accurate for smaller temperature differences and reasonable, for example, when the wall temperature is close to the bulk temperature later in the downcomer cooling process during a PTS event.

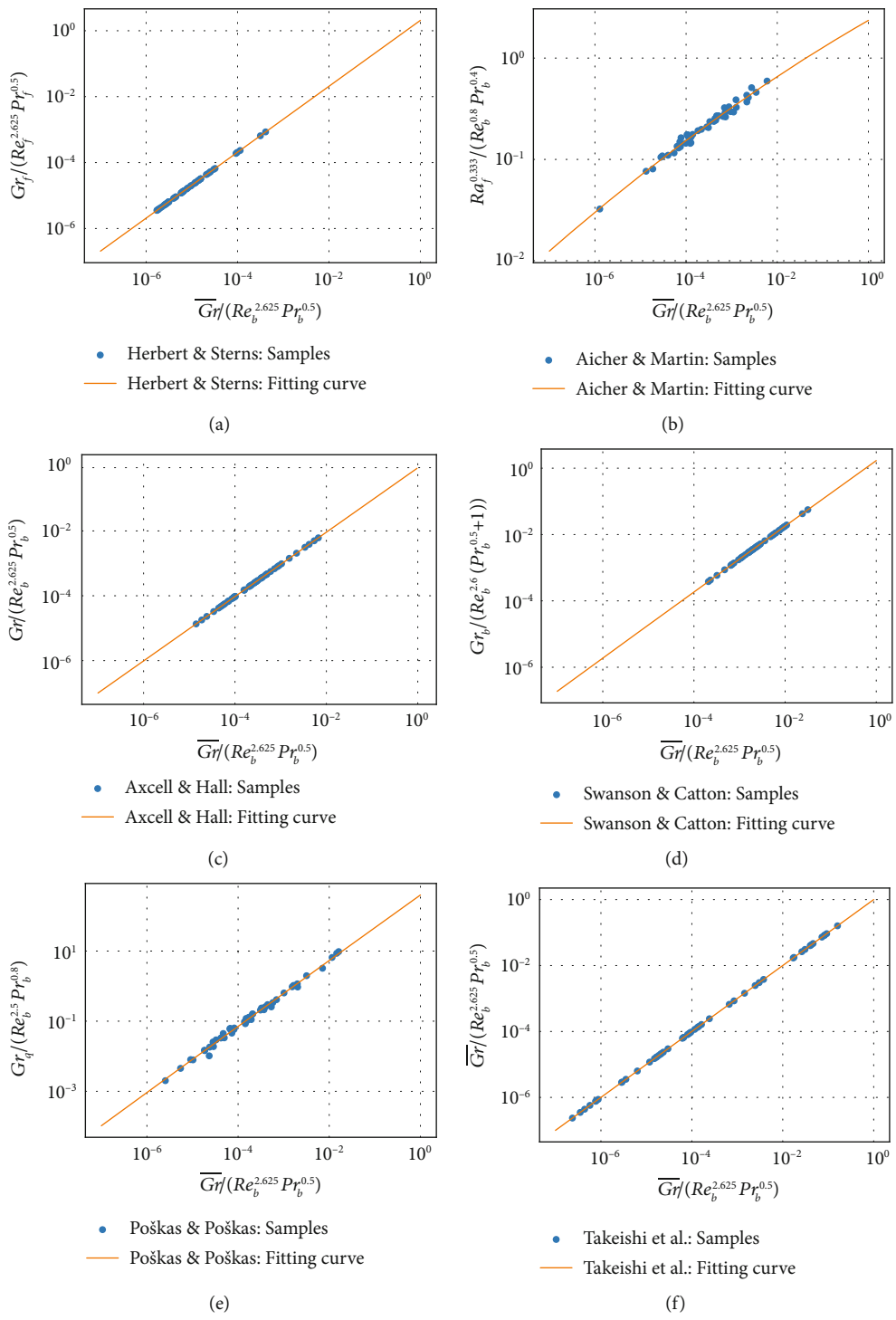

Figure 10: Relationship between Jackson and Fewster's dependent parameter $\overline{\mathrm{Gr}}/(\mathrm{Re}_b^{2.625}\mathrm{Pr}_b^{0.5})$ and the dependent parameters for (a) Herbert and Sterns [20], (b) Aicher and Martin [1], (c) Axcell and Hall [34], (d) Swanson and Catton (IJHMT) [15], (e) P. Poskas and R. Poskas [16], and (f) Takeshi et al. [51] for the sample calculation conditions used in Section 3.1. Solid lines show the fitting curves. Although the channel geometries, the parameter ranges, and the working fluids differ, all sampling data distributed along a line.

For example, when the working fluid is water, the bulk temperature is $T_b = 300\,\mathrm{K}$, and the temperature difference is $T_w - T_b = 20\,\mathrm{K}$; the nondimensional numbers can be approximated as $\mathrm{Pr}_b = 1.25\mathrm{Pr}_f$, $\mathrm{Re}_b = 0.82\mathrm{Re}_f$, $\mathrm{Gr}_b = 0.53\mathrm{Gr}_f$, and $\mathrm{Gr}_b = 1.70\overline{\mathrm{Gr}}$. Based on the proportionalities, $\mathrm{Nu}_{\mathrm{ft}} \sim \mathrm{Re}^{0.8}\mathrm{Pr}^{0.4}$ and $\mathrm{Nu}_{\mathrm{nt}} \sim \mathrm{Gr}^{0.333}\mathrm{Pr}^{0.333}$, the maximum influence of the approximation on Nu can be estimated to be 9% for forced convection and 9%–15% for natural convection. These approximations are reasonable for qualitatively evaluating the asymptotic behavior. The nondimensional numbers are sampled from the range shown in Table 10. The horizontal axis is Jackson and Fewster's dependent parameter. The vertical axis is $\mathrm{Nu}/\mathrm{Nu}_{\mathrm{ft}}$ for Figure 12(a) and $\mathrm{Nu}/\mathrm{Nu}_{\mathrm{nt}}$ for Figure 12(b). The Gnielinski (Eqs. (37a) and (37b)) and the Churchill and Chu (Eq. (9)) correlations are used for $\mathrm{Nu}_{\mathrm{ft}}$ and $\mathrm{Nu}_{\mathrm{nt}}$, respectively. These correlations can apply within the whole range, where the parameters are sampled (Table 10) [17]. Figure 12(a) shows that $\mathrm{Nu} \approx \mathrm{Nu}_{\mathrm{ft}}$ for $\mathrm{Gr}/\mathrm{Re}^{2.625}\mathrm{Pr}^{0.5} < 10^{-4}$, indicating that turbulent forced convection is dominant. Figure 12(b) shows that $\mathrm{Nu} \approx \mathrm{Nu}_{\mathrm{nt}}$ for $\mathrm{Gr}/\mathrm{Re}^{2.625}\mathrm{Pr}^{0.5} > 10^{-2}$, indicating that turbulent natural convection is dominant. The mixed convection conditions are in the range of $10^{-4} \le \mathrm{Gr}/\mathrm{Re}^{2.625}\mathrm{Pr}^{0.5} \le 10^{-2}$. Figure 12(a) shows that all correlations provide good predictions under forced convection conditions, which is obvious for most correlations because they are modeled to approach the forced convection correlations under forced convection-dominant conditions. Figure 12(b) shows that the Aicher and Martin and Churchill correlations are excellent in prediction under the natural convection-dominant conditions because they are the interpolation formulas. Although the Jackson and Fewster correlation is not an interpolation equation, it is excellent in prediction under the natural convection-dominant condition because it has a similar functional form under the natural convection-dominant condition (Appendix D). These correlations can apply in a wider range of conditions than those validated experimentally by the correlation developers. Predictions by the Swanson and Catton (JHT) correlation are widely scattered compared to the other correlations because it does not include the dependency on Pr. Furthermore, since the Swanson and Catton (JHT) and Swanson and Catton (IJHMT) correlations are not interpolation formulas and the difference between Nu and $\mathrm{Nu}_{\mathrm{nt}}$ slightly increases for the large dependent parameter, the range of application should receive attention.

4.4. Correlation Applicability to Conditions Assuming LBLOCA in Actual Plants. In Section 4.3, the authors discussed the extrapolation performance of the mixed convection correlations with respect to forced and natural convection by sampling the nondimensional numbers under various conditions. In this section, the authors investigate the applicability of the mixed convection correlations to forced and natural convection conditions under conditions assuming LBLOCA in an actual plant as an example. Table 11 shows the parameter ranges assumed in this analysis. The assumptions are as follows. The working fluid is water with a bulk temperature of 300 K at atmospheric pressure, a condition that

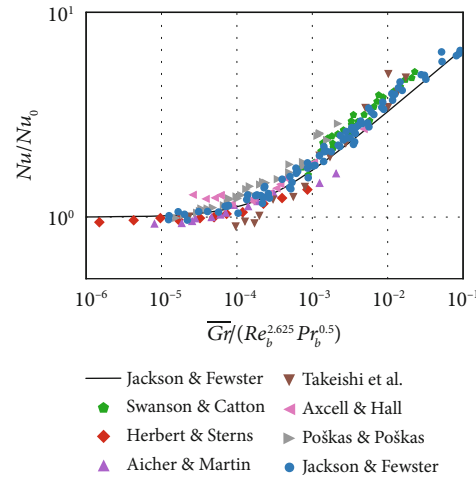

FIGURE 11: The $\mathrm{Nu}/\mathrm{Nu}_0$ as a function of $\overline{\mathrm{Gr}}/(\mathrm{Re}_b^{2.625}\,\mathrm{Pr}_b^{0.5})$. The solid line shows the Jackson and Fewster correlation (Eq. (15)). The symbols are the experimental data with respect to Jackson and Fewster [13], Swanson and Catton [15], Herbert and Sterns [20], Aicher and Martin [1], Takeishi et al. [51], Axcell and Hall [34], and P. Poskas and R. Poskas [16].

can occur during the LBLOCA. The wall temperature range is shown in Table 11, assuming that the single-phase mixed convection correlations are applied where the wall temperature is lower than 373 K. The characteristic length D_h is chosen with reference to the UPTF experiment [52]: a 1:1 representation of a PWR primary system. Table 11 shows the Grashof number ranges calculated from ΔT obtained by random sampling. The range of Re_b shown in Table 11 is determined as a sufficiently wide range under turbulent conditions. Randomly selected Re_b from this range gives the characteristic velocity. Table 12 shows the mean $\bar{\epsilon}$ and the standard deviation σ_ϵ of the percentage error ϵ_i and mean absolute percentage error $\bar{\epsilon}_r$ when comparing $\mathrm{Nu}_{\mathrm{mt}}$, obtained from each mixed convection correlation, with FC the turbulent forced $\mathrm{Nu}_{\mathrm{ft}}$ and NC the natural $\mathrm{Nu}_{\mathrm{nt}}$ correlation. The reference values $\mathrm{Nu}_{\mathrm{ft}}$ and $\mathrm{Nu}_{\mathrm{nt}}$ are calculated using the Gnielinski (Eqs. (37a) and (37b)) and Churchill and Chu correlations (Eq. (9)), respectively.

$$\epsilon_i = \frac{\mathrm{Nu}_{\mathrm{mt}} - \mathrm{Nu}_{(\mathrm{ft}|\mathrm{nt})}}{\mathrm{Nu}_{(\mathrm{ft}|\mathrm{nt})}}, \tag{50a}$$

$$\bar{\epsilon} = \frac{1}{N}\sum_{i=1}^{N}\epsilon_i, \tag{50b}$$

$$\bar{\epsilon}_r = \frac{1}{N}\sum_{i=1}^{N}|\epsilon_i|, \tag{50c}$$

$$\sigma_\epsilon = \sqrt{\frac{1}{N}\sum_{i=1}^{N}|\epsilon_i - \bar{\epsilon}|^2}, \tag{50d}$$

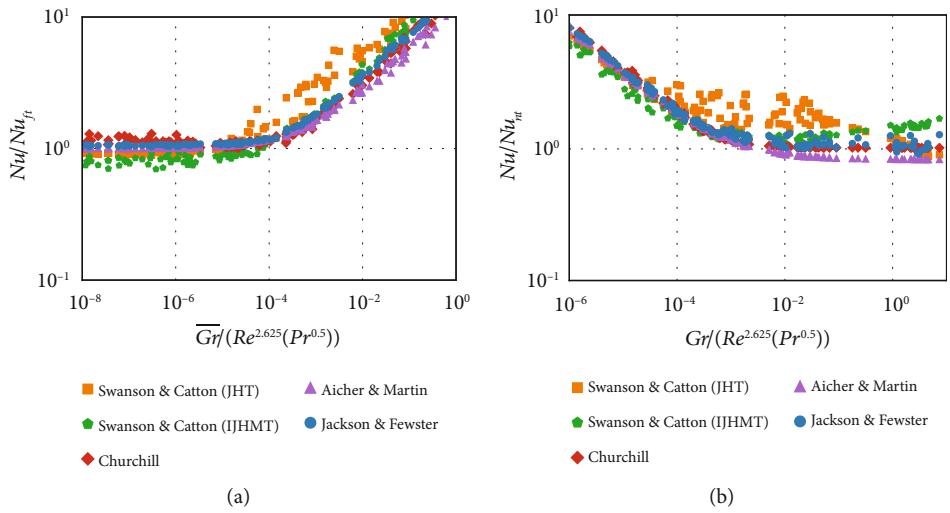

Figure 12: The ratio of the mixed convection heat transfer coefficient to (a) the forced Nu/Nu_{ft} and (b) natural convection ones Nu/Nu_{nt}, where the correlations for Nu_{ft} and Nu_{nt} are calculated using Gnielinski (Eqs. (37a) and (37b)) and Churchill and Chu (Eq. (9)), respectively. Nondimensional numbers are randomly sampled in the range of Table 10.

Table 10: The range of nondimensional numbers for data sampling.

Prandtl number Pr	0.7–7.0
Reynolds number Re	$10^4 - 5 \times 10^6$
Grashof number Gr	$10^9 - 10^{13}$

Table 11: The test calculation conditions used to verify the extrapolation for the mixed convection heat transfer correlations.

Working fluid	Water
Pressure P (MPa)	0.1
Wall temperature T_w (K)	300–373
Bulk temperature T_b (K)	300
Hydraulic diameter D_h (cm)	50
Reynolds number Re_b	10^4–10^7
Grashof number Gr_b	$8.34 \times 10^8 < Gr_b < 3.37 \times 10^{10}$, $4.25 \times 10^8 < \bar{Gr} < 2.76 \times 10^{10}$, $8.93 \times 10^8 < Gr_f < 2.38 \times 10^{11}$

where $Nu_{(ft|nt)}$ indicates the reference Nusselt numbers: Nu_{ft} or Nu_{nt}. The mean absolute percentage errors for the Jackson and Fewster, Aicher and Martin, and Churchill correlations are lower than 15% for the forced and natural convection-dominant conditions, indicating the excellent applicability of these correlations.

Table 12: Mean ($\bar{\epsilon}$) and standard deviation (σ_ϵ) for the percentage error and mean absolute percentage error $\bar{\epsilon}_r$.

		$\bar{\epsilon}$ (%)	σ_ϵ (%)	$\bar{\epsilon}_r$ (%)
SC (JHT)	FC	15.3	5.2	15.6
	NC	-17.6	14.1	19.5
SC (IJHMT)	FC	25.7	9.2	25.7
	NC	-1.0	9,9	7.7
JF	FC	3.4	2.6	4.1
	NC	7.7	5.5	8.7
AM	FC	-2.4	4.1	2.4
	NC	13.1	1.5	13.1
Ch	FC	-6.8	10.0	9.9
	NC	-0.3	0.2	0.3

FC: forced convection; NC: natural convection. SC (JHT), SC (IJHMT), JF, AM, and Ch represent Swanson and Catton JHT (Eq. (24)), Swanson and Catton IJHMT (Eq. (30)), Jackson and Fewster (Eq. (15)), Aicher and Martin (Eq. (19)), and Churchill (Eq. (7)), respectively.

5. Conclusions

This study was conducted to gain a comprehensive understanding of opposing flow mixed convection heat transfer and to establish the prediction methodology by evaluating existing correlations and models. An extensive review of existing data and correlations was conducted to develop the database and the correlation bank to achieve the objectives. The review revealed that straightforward comparisons between existing data and correlations were not possible because nondimensional parameters in the databases and the correlations were not uniquely defined. The authors developed a methodology to generate essential thermofluid

parameters necessary for model evaluation from nondimensional parameters available in the literature based on boundary conditions and random sampling. The developed methodology allowed us to perform detailed evaluations of available correlations and models, including the extrapolation performance of each correlation and model to two limiting cases, such as forced and natural convection flows. The in-depth analyses revealed the effect of the experimental conditions, such as the thermal boundary conditions, the channel geometries, the working fluids, and the heating wall, on opposing flow mixed convection heat transfer. The obtained results are summarized as follows.

(i) The Jackson and Fewster, Churchill, and Swanson and Catton (IJHMT) correlations can predict existing experimental data with the parameter ranges summarized in Tables 3–9 with high accuracy

(ii) The difference in the thermal boundary conditions, i.e., UWT and UHF, does not affect the heat transfer coefficient in the case of mixed convection similar to the case of forced and natural convections

(iii) The differences in the channel geometry and the working fluid can be generalized using the hydraulic-equivalent diameter and appropriate nondimensional numbers, respectively, and the existing correlations can predict the heat transfer coefficient regardless of the differences in the channel geometries and working fluids

(iv) No substantial difference is observed between the mixed convection heat transfer coefficients for one- and two-side heating. Thus, the existing correlations can predict heat transfer coefficients without being affected by the asymmetric heating conditions

(v) The authors evaluated the applicability of the mixed convection correlations with respect to forced and natural convection-dominant conditions under a wide nondimensional number ranges than that validated based on the experiments conducted in the previous studies. Consequently, the Jackson and Fewster, Churchill, and Aicher and Martin correlations asymptotically approach the forced and natural convection heat transfer correlations under the two dominant conditions, indicating the excellent extrapolation ability. Hence, the correlations could be applied beyond the parameter ranges validated based on experiments conducted in the previous studies

(vi) The Jackson and Fewster, Aicher and Martin, and Churchill correlations have excellent predictive performance under natural and forced convection-dominant conditions assuming LBLOCA in actual plants

Appendix

A. Shear Stress Distribution for Mixed Convection Opposing Flow near a Heated Wall

The authors assume the presence of fully developed turbulent mixed convection opposing flow in a circular tube. The force balance among the pressure gradient, buoyancy, and viscous shear stress τ from a heated wall (Figure 13) to an arbitrary distance y is given by

$$0 = -\pi\left[R^2 - (R-y)^2\right]\frac{dp}{dx} - 2\pi g\int_0^y (\rho_b - \rho)\left(R - y'\right)dy' - 2\pi R\tau_w + 2\pi(R-y)\tau, \tag{A.1}$$

where R is the tube radius and p is the pressure. When $y = R$, Eq. (A.1) can be expressed as follows for the entire tube.

$$\frac{dp}{dx} = \frac{1}{\pi R^2}\left[-2\pi g\int_0^R (\rho_b - \rho)\left(R - y'\right)dy' - 2\pi R\tau_w\right]. \tag{A.2}$$

Substituting Eq. (A.2) into Eq. (A.1) to eliminate the pressure gradient term, the authors obtain

$$\left[1 - \left(1 - \frac{y}{R}\right)^2\right]\left[-2\pi g\int_0^R (\rho_b - \rho)\left(R - y'\right)dy' - 2\pi R\tau_w\right] = -2\pi g\int_0^y (\rho_b - \rho)\left(R - y'\right)dy' - 2\pi R\tau_w + 2\pi(R-y)\tau. \tag{A.3}$$

Near the heated wall ($y/R \ll 1$), the above equation becomes

$$\tau = \tau_w + g\int_0^y (\rho_b - \rho)dy'. \tag{A.4}$$

When $y = \delta_T$, the authors finally obtain

$$\Delta\tau = \tau - \tau_w = \int_0^{\delta_T} (\rho_b - \rho)g dy. \tag{A.5}$$

B. Derivation of Jackson and Fewster's Dependent Parameter

Jackson and Fewster [13] derived the dependent parameter by considering the nondimensionalization of Eq. (10). This appendix reviews the derivation procedure of the dependent parameter. Majority of the thermal resistance to a turbulent flow is in a thermal boundary layer near a heated wall. Moreover, the heat transfer coefficient h is inversely proportional to the thermal boundary layer thickness δ_T: $h \sim \delta_T^{-1}$. For forced convective heat transfer, Jackson and Fewster assumed that h is proportional to $\mathrm{Pr}_b^{0.5}$: $h = \mathrm{const.Pr}_b^{0.5}$. The proportionality constant was determined based on the

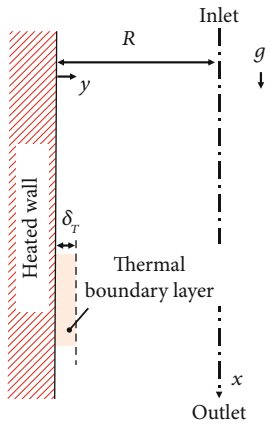

Figure 13: Schematic of the thermal boundary layer.

relationship that the thermal boundary layer has a similar thickness as the velocity boundary layer for $\mathrm{Pr}_b = 1$, i.e., $\delta_T \approx \delta_M$, and the following relationship between δ_T and δ_M was derived.

$$\delta_T = \delta_M \, \mathrm{Pr}_b^{-0.5}. \tag{B.1}$$

Furthermore, δ_M^+ becomes a constant independent of Re_b when nondimensionalized as $\delta_M^+ = \delta_M (\tau_w \rho_b)^{0.5} / \mu_b$ using the wall coordinate. Dividing Eq. (10) by τ_w and substituting Eq. (B.1) into it, Jackson and Fewster obtained

$$\frac{\Delta\tau}{\tau_w} \approx \frac{2\sqrt{2}\,\delta_M^+ \bar{\mathrm{Gr}}}{\mathrm{Re}_b^3 \, c_f^{1.5} \, \mathrm{Pr}_b^{0.5}}. \tag{B.2}$$

Assuming $c_f \sim \mathrm{Re}_b^{-0.25}$, Jackson and Fewster obtained the following with a proportionality constant K_1.

$$\frac{\Delta\tau_{\delta_b}}{\tau_w} \approx K_1 \frac{\bar{\mathrm{Gr}}}{\mathrm{Re}_b^{2.625} \, \mathrm{Pr}_b^{0.5}}. \tag{B.3}$$

For turbulent forced convection, $\bar{\mathrm{Gr}}/\mathrm{Re}_b^{2.625} \, \mathrm{Pr}_b^{0.5}$ is the fundamental dependent parameter.

For turbulent natural convection, $\delta_T = \mathrm{const.} D \, \mathrm{Ra}_b^{-1/3}$ is derived based on the proportionality $\mathrm{Nu}_b \sim \mathrm{Ra}_b^{1/3}$. Dividing Eq. (10) by τ_w and substituting $\delta_T = \mathrm{const.} D \, \mathrm{Ra}_b^{-1/3}$ into it, Jackson and Fewster obtained the following equation using the proportionality constant K_2.

$$\frac{\Delta\tau}{\tau_w} = K_2 \left(\frac{\bar{\mathrm{Gr}}}{\mathrm{Re}_b^{2.625} \mathrm{Pr}_b^{0.5}} \right)^{2/3}. \tag{B.4}$$

Moreover, $\bar{\mathrm{Gr}}/\mathrm{Re}_b^{2.625} \, \mathrm{Pr}_b^{0.5}$ is the dependent parameter for turbulent natural convection. $\bar{\mathrm{Gr}}/\mathrm{Re}_b^{2.625} \, \mathrm{Pr}_b^{0.5}$ is the dependent parameter for natural and forced convections, indicating that it is also the dependent parameter for turbulent mixed convection.

C. Discussion on Exponents and Dependent Parameter in the Jackson and Fewster Correlation

During the process of deriving the dependent parameter $\bar{\mathrm{Gr}}/\mathrm{Re}_b^{2.625} \, \mathrm{Pr}_b^{0.5}$ (Appendix B), Jackson and Fewster [13] assumed that the Nusselt number $\mathrm{Nu}_{0,b}$ and the friction coefficient c_f for forced convection are proportional to $\mathrm{Re}_b^{0.82}$ and $\mathrm{Re}_b^{-0.25}$, respectively. This assumption affects the dependent parameter and the exponent 0.47 in Eq. (14). For example, if the authors assume $u_{0,b} \sim \mathrm{Re}_b^{0.8}$ and $c_f \sim \mathrm{Re}_b^{-0.20}$, the dependent parameter becomes $\overline{\mathrm{Gr}}/\mathrm{Re}_b^{2.7} \, \mathrm{Pr}_b^{0.5}$ [24], and the authors obtain the following equation instead of Eq. (13).

$$\frac{h'}{h_0} = \left(\frac{\tau_w'}{\tau_w} \right)^{0.444}. \tag{C.1}$$

The exponent of this equation is slightly smaller than that of Eq. (13). Finally, Jackson and Fewster adjusted the exponent to 0.31 to ensure that Nu_b does not depend on Re_b under natural convection-dominant conditions. Assuming the proportionality $\mathrm{Nu}_{0,b} \sim \mathrm{Re}_b^{0.8}$ and $c_f \sim \mathrm{Re}_b^{-0.20}$ and modifying the exponent for Nu_b to not depend on Re_b, the exponent becomes 0.29. Because Re_b for each experimental condition is available in Jackson and Fewster's study, the dependent parameter $\bar{\mathrm{Gr}}/\mathrm{Re}_b^{2.625} \, \mathrm{Pr}_b^{0.5}$ can be transformed to $\overline{\mathrm{Gr}}/\mathrm{Re}_b^{2.7} \, \mathrm{Pr}_b^{0.5}$. The correlation with the dependent parameter $\overline{\mathrm{Gr}}/\mathrm{Re}_b^{2.7} \, \mathrm{Pr}_b^{0.5}$, the exponent 0.29, and the model constant evaluated based on Jackson and Fewster's experimental data is expressed as follows.

$$\frac{\mathrm{Nu}_b}{\mathrm{Nu}_{0,b}} = \left(1 + 11903 \frac{\overline{\mathrm{Gr}}}{\mathrm{Re}_b^{2.7} \mathrm{Pr}_b^{0.5}} \right)^{0.29}. \tag{C.2}$$

The difference between predictions based on the original Jackson and Fewster correlation (Eq. (15)) and the modified correlation (Eq. (C.2)) is less than ~20% under mixed convection conditions, i.e., $10^{-4} < \bar{\mathrm{Gr}}/\mathrm{Re}_b^{2.625} \, \mathrm{Pr}_b^{0.5} < 10^{-2}$ and $10^4 \leq \mathrm{Re}_b \leq 10^7$, demonstrating that the small difference between exponents does not affect the predictivity substantially.

D. Extrapolation Performance of Jackson and Fewster's Correlation under Natural Convection Dominant Conditions

The Jackson and Fewster correlation (Eq. (15)), which is a mixed convection heat transfer correlation, has the same predictivity as natural convection heat transfer correlations under natural convection-dominant conditions. For the sake of simplicity, the authors assume that the fluid bulk temperature is 300 K and the working fluid is water ($\mathrm{Pr}_b = 5.86$) at atmospheric pressure. Then, the following interpolation formula can be applied for mixed convection heat transfer coefficients [17].

$$\mathrm{Nu}^{\gamma} = \mathrm{Nu}_{\mathrm{nt}}^{\gamma} + \mathrm{Nu}_{\mathrm{ft}}^{\gamma}. \quad (D.1)$$

Turbulent mixed convections frequently use $\gamma = 3$, which is also adopted in the Churchill correlation (Eq. (7)). The authors transform Eq. (D.1) to

$$\frac{\mathrm{Nu}}{\mathrm{Nu}_{\mathrm{ft}}} = \left\{1 + \left(\frac{\mathrm{Nu}_{\mathrm{nt}}}{\mathrm{Nu}_{\mathrm{ft}}}\right)^{\gamma}\right\}^{1/\gamma}. \quad (D.2)$$

The authors obtain the following equation considering $\gamma = 1/0.31 \approx 3.23$.

$$\mathrm{Nu}_{\mathrm{nt}} = \mathrm{Nu}_{\mathrm{ft}}\left(4500\frac{\overline{\mathrm{Gr}}}{\mathrm{Re}_b^{2.625}\,\mathrm{Pr}_b^{0.5}}\right)^{0.31}. \quad (D.3)$$

The Jackson and Fewster correlation indicates that Eq. (15) converges into Eq. (D.3) under natural convection-dominant conditions. Jackson and Fewster multiplied the Petukhov and Kirrilov correlation (Eqs. (16a) and (16b)) by 1.16 to obtain a forced convection heat transfer correlation $\mathrm{Nu}_{\mathrm{ft}}$. However, herein, the authors use the Dittus and Boelter correlation (Eq. (45)) to facilitate the analytical treatment. The authors multiply Eq. (45) by 1.29 to reduce the difference between Dittus and Boelter and the Petukhov and Kirrilov correlations. Even if the authors modify the $\mathrm{Nu}_{\mathrm{ft}}$ correlation in the abovementioned manner, the error is <3.6% under Jackson and Fewster's experimental conditions. Substituting the Dittus and Boelter equation multiplied by 1.29 into Eq. (D.3), the authors obtain

$$\mathrm{Nu}_{\mathrm{nt}} \approx \frac{0.40}{\mathrm{Pr}_b^{0.065}\mathrm{Re}_b^{0.01375}}\left(\overline{\mathrm{Gr}}\,\mathrm{Pr}_b\right)^{0.31}. \quad (D.4)$$

Even when the authors consider $\mathrm{Re}_b^{0.01375} \approx 0.89$ under Jackson and Fewster's experimental conditions, the error is <2.2%. The approximation $\overline{\mathrm{Gr}} \approx 0.3\,\mathrm{Gr}_f$ is reasonable for the typical temperature difference range. Finally, substituting these values in Eq. (D.4), the Jackson and Fewster correlation can be approximated using the following equation under natural convection-dominant conditions.

$$\mathrm{Nu}_{\mathrm{nt}} \approx 0.218\,\mathrm{Ra}_f{}^{0.31}. \quad (D.5)$$

Then, the Churchill and Chu correlation (Eq. (9)) becomes

$$\mathrm{Nu}_{\mathrm{nt}} \approx 0.13\,\mathrm{Ra}_f^{0.333}. \quad (D.6)$$

This equation is the McAdams correlation (Eq. (40b)) [53] implemented in the TRACE code. In the range of $10^9 \le \mathrm{Ra}_f \le 10^{13}$, even if the authors assume $\mathrm{Ra}_f{}^{0.31}/\mathrm{Ra}_f^{0.333} = \mathrm{Ra}_f^{-0.02333} \approx 0.55$, the error is <10%. Therefore, Eq. (D.5) can be expressed as

$$\mathrm{Nu}_{\mathrm{nt}} \approx 0.12\,\mathrm{Ra}_f{}^{0.333}. \quad (D.7)$$

Comparing Eq. (D.7) and Eq. (D.6) demonstrates that the Jackson and Fewster correlation gives a similar prediction as the natural convection heat transfer correlations under natural convection-dominant conditions. Selby [54] obtained similar conclusions using the data from the experiments conducted using air as the fluid by Brdlik et al. [55].

Data Availability

The data used to support the findings of this study are available from the corresponding authors upon request.

Disclosure

This study was conducted under the contract with the Nuclear Regulation Authority (NRA) of Japan.

Conflicts of Interest

The authors declare that they have no conflicts of interest.

Acknowledgments

One of the authors (T. Hibiki) would like to express his sincere appreciation to the Hong Kong SAR government and Hong Kong Jockey Club for supporting his research under the Global STEM Professorship and JC STEM Lab of Innovative Thermal-fluid Science, respectively.

References

[1] T. Aicher and H. Martin, "New correlations for mixed turbulent natural and forced convection heat transfer in vertical tubes," *International Journal of Heat and Mass Transfer*, vol. 40, no. 15, pp. 3617–3626, 1997.

[2] Nuclear Regulatory Commission Division of Systems Technology, *RELAP5/MOD3.3 Code Manual Volume IV: Models and Correlations*, Washington, DC (United States), 2001, https://inis.iaea.org/search/search.aspx?orig_q=RN:27019719.

[3] J. W. Spore, J. S. Elson, S. J. Jolly-Woodruff et al., "TRAC-M/FORTRAN 90 (Version 3.0) Theory Manual," 2001, https://www.nrc.gov/reading-rm/doc-collections/nuregs/contract/cr6724/index.html#pub-info.

[4] U. S. Nuclear Regulatory Commission, *TRACE V5.0 Patch 6 Theory Manual Field Equations, Solution Methods, and Physical Models*, U. S. Nuclear Regulatory Commission, 2020.

[5] P. Emonot, A. Souyri, J. L. Gandrille, and F. Barré, "CATHARE-3: a new system code for thermal-hydraulics in the context of the NEPTUNE project," *Nuclear Engineering and Design*, vol. 241, pp. 4476–4481, 2011.

[6] Gesellschaft fuer Anlagen- und Reaktorsicherheit (GRS) gGmbH, *ATHLET 3.1A Program Overview*, Gesellschaft fuer Anlagen- und Reaktorsicherheit (GRS) gGmbH, 2016.

[7] N. H. Hoang, Y. K. Kwack, S. H. Bae, Y. S. Kim, and S. K. Sim, "Improvement of MARS-KS sub-channel module using CTF code," *Nuclear Engineering and Design*, vol. 358, article 110431, 2020.

[8] J. Kaneko and N. Tsukamoto, "Analytical functions and development status of the system analysis code for nuclear power

plants, AMAGI," *Transactions of the Atomic Energy Society of Japan*, vol. 19, no. 3, pp. 163–177, 2020.

[9] D. R. Liles and J. H. Mahaffy, *TRAC-PF1/MOD1: An Advanced Best-Estimate Computer Program for Pressurized Water Reactor Thermal-Hydraulic Analysis*, Los Alamos National Laboratory (LANL), NM, 1986.

[10] J. A. Borkowski, N. L. Wade, S. Z. Rouhani et al., *TRAC-BF1/MOD1 Models and Correlations, NUREG/CR-4391; EGG-2680*, U. S. Nuclear Regulatory Commission, United States, 1992.

[11] L. W. Swanson and I. Catton, "Enhanced heat transfer due to secondary flows in mixed turbulent convection," *Journal of Heat Transfer*, vol. 109, no. 4, pp. 943–946, 1987.

[12] Japan Electric Association, *Verification Method of Fracture Toughness for In-service Reactor Pressure Vessel, JEAC4206-2007*, Japan Electric Association, 2007.

[13] J. D. Jackson and J. Fewster, "Enhancement of heat transfer due to buoyancy for downward flow of water in vertical tubes," *Heat Transfer and Turbulent Buoyant Convection: Studies and Applications for Natural Environment, Buildings, Engineering Systems; Proceedings of the Seminar*, vol. 1 and 2, 1977, pp. 759–775, Hemisphere Publishing Corporation, Washington, D.C., Dubrovnik, Yugoslavia, 1976.

[14] S. W. Churchill, "Combined free and forced convection in channels," in *Heat Exchanger Design Handbook*, E. U. Schlunder, Ed., Hemisphere Publishing Corporation, Washington, DC (United States), 1983.

[15] L. W. Swanson and I. Catton, "Surface renewal theory for turbulent mixed convection in vertical ducts," *International Journal of Heat and Mass Transfer*, vol. 30, no. 11, pp. 2271–2279, 1987.

[16] P. Poskas and R. Poskas, "Turbulent opposing mixed convection heat transfer in a vertical flat channel with one-side heating," *Heat Transfer Engineering*, vol. 25, no. 2, pp. 17–23, 2004.

[17] F. P. Incropera, D. P. DeWitt, T. L. Bergman, and A. S. Lavine, *Fundamentals of Heat and Mass Transfer*, Wiley, New York, 2006.

[18] S. W. Churchill, "Comprehensive correlating equations for heat, mass and momentum transfer in fully developed flow in smooth tubes," *Industrial and Engineering Chemistry Fundamentals*, vol. 16, no. 1, pp. 109–116, 1977.

[19] S. W. Churchill and H. H. S. Chu, "Correlating equations for laminar and turbulent free convection from a vertical plate," *International Journal of Heat and Mass Transfer*, vol. 18, no. 11, pp. 1323–1329, 1975.

[20] L. S. Herbert and U. J. Sterns, "Heat transfer in vertical tubes-interaction of forced and free convection," *The Chemical Engineering Journal*, vol. 4, no. 1, pp. 46–52, 1972.

[21] G. U. Kang and B. J. Chung, "The experimental study on transition criteria of natural convection inside a vertical pipe," *International Communications in Heat and Mass Transfer*, vol. 37, no. 8, pp. 1057–1063, 2010.

[22] W. M. Yan and T. F. Lin, "Theoretical and experimental study of natural convection pipe flows at high Rayleigh number," *International Journal of Heat and Mass Transfer*, vol. 34, no. 1, pp. 291–303, 1991.

[23] S. M. Ohk and B. J. Chung, "Natural convection heat transfer inside an open vertical pipe: influences of length, diameter and Prandtl number," *International Journal of Thermal Sciences*, vol. 115, pp. 54–64, 2017.

[24] W. B. Hall and J. D. Jackson, "Laminarization of a turbulent pipe flow by buoyancy forces," in *ASME 11th National Heat Transfer Conferenc, No. 69-HT-55., ASME*, New York, New York, 1969.

[25] B. S. Petukhov and V. V. Kirillov, "The problem of heat exchange in the turbulent flow of liquids in tubes," *Teploenergetika*, vol. 4, no. 4, pp. 63–68, 1958.

[26] D. D. Joye, "Comparison of aiding and opposing mixed convection heat transfer in a vertical tube with Grashof number variation," *International Journal of Heat and Fluid Flow*, vol. 17, no. 2, pp. 96–101, 1996.

[27] D. D. Joye, "Design criterion for the heat-transfer coefficient in opposing flow, mixed convection heat transfer in a vertical tube," *Industrial and Engineering Chemistry Research*, vol. 35, no. 7, pp. 2399–2403, 1996.

[28] V. Gnielinski, "Ein neues Berechnungsverfahren für die Wärmeübertragung im Übergangsbereich zwischen laminarer und turbulenter Rohrströmung," *Forschung im Ingenieurwesen*, vol. 61, no. 9, pp. 240–248, 1995.

[29] V. Gnielinski, "Zur Wärmeübertragung bei laminarer Rohrströmung und konstanter Wandtemperatur," *Chemie Ingenieur Technik*, vol. 61, no. 2, pp. 160-161, 1989.

[30] A. Temu, W. Blumberg, V. Gnielinski, and H. Martin, "Überlagerte erzwungene und freie Konvektion in einem senkrechten Rohr. Wiss. Abschlu ber," in *International Seminar d*, pp. 49–58, Univ. Karlsruche, University of Karlsruch, 1989.

[31] P. E. Saylor and D. D. Joye, *Pressure Drop in Mixed Convection Heat Transfer in Vertical Tube*, Research proposal, Villanova University, Villanova, PA, 1988.

[32] R. H. Norris and M. W. Sims, "A simplified heat transfer correlation for semi-turbulent flow of liquids in pipes," *Transactions AIChE*, vol. 38, pp. 469–492, 1942.

[33] A. Watzinger and D. G. Johnson, "Wärmeübertragung von Wasser an Rohrwand bei senkrechter Strömung im Übergangsgebiet zwischen laminarer und turbulenter Strömung," *Forschung Auf Dem Gebiete Des Ingenieurwesens*, vol. 10, no. 4, pp. 182–196, 1939.

[34] B. P. Axcell and W. B. Hall, "Mixed convection to air in a vertical pipe," in *Proceeding of International Heat Transfer Conference 6*, pp. 37–42, Begellhouse, Connecticut, 1978.

[35] I. Catton and L. Swanson, *Mixed Turbulent Convective Heat Transfer in Certical Ducts*, Electric Power Research Institute, 1988.

[36] P. V. Danckwerts, "Significance of liquid-film coefficients in gas absorption," *Industrial & Engineering Chemistry*, vol. 43, pp. 1460–1467, 1951.

[37] T. J. Hanratty, "Turbulent exchange of mass and momentum with a boundary," *AIChE Journal*, vol. 2, no. 3, pp. 359–362, 1956.

[38] L. C. Thomas and M. L. Wood, "A new approach to the analysis of turbulent free convection heat transfer," *International Journal of Heat and Fluid Flow*, vol. 1, no. 2, pp. 93–96, 1979.

[39] L. C. Thomas and C. R. Kakarala, "A unified model for turbulent and laminar momentum transfer: channel flow," *Transactions ASME*, vol. 43, no. 1, pp. 8–12, 1976.

[40] L. C. Thomas, B. T. F. Chung, and S. K. Mahaldar, "Temperature profiles for turbulent flow of high prandtl number fluids," *International Journal of Heat and Mass Transfer*, vol. 14, no. 9, pp. 1465–1471, 1971.

[41] J. Vilemas, B. Cesna, and V. Survila, *Heat Transfer in Gas-Cooled Annular Channels*, Hemisphere Publishing, United States, 1987.

[42] B. S. Petukhov and L. I. Roizen, "Generalized relationships for heat transfer in turbulent flow of gas in tubes of annular section," *High Temperature*, vol. 2, pp. 65–68, 1964.

[43] J. R. Sellars, M. Tribus, and J. S. Klein, "Heat transfer to laminar flow in a round tube or flat conduit—the Graetz problem extended," *Journal of Fluids Engineering*, vol. 78, no. 2, pp. 441–447, 1956.

[44] V. Gnielinski, "New equations for heat and mass transfer in turbulent pipe and channel flow," *International Chemical Engineering*, vol. 16, pp. 359–368, 1976.

[45] W. Hufschmidt and E. Burck, "Der einfluss temperaturabhängiger stoffwerte auf den wärmeübergang bei turbulenter strömung von flüssigkeiten in rohren bei hohen wärmestromdichten und prandtlzahlen," *International Journal of Heat and Mass Transfer*, vol. 11, no. 6, pp. 1041–1048, 1968.

[46] W. Elenbaas, "Heat dissipation of parallel plates by free convection," *Physica*, vol. 9, no. 1, pp. 1–28, 1942.

[47] W. Elenbaas, "The dissipation of heat by free convection the inner surface of vertical tubes of different shapes of cross-section," *Physica*, vol. 9, no. 8, pp. 865–874, 1942.

[48] B. Lee, S.-K. Park, A. Shin, M. K. Cho, and K. Tien, "NUREG/IA-0508- "International Agreement Report-Validation of RELAP5/MOD3.3 Friction Loss and Heat Transfer Model for Narrow Rectangular Channels"," https://www.nrc.gov/reading-rm.html.

[49] B. S. Petukhov, "Heat transfer and friction in turbulent pipe flow with variable physical properties," *Advances in Heat Transfer*, vol. 6, pp. 503–564, 1970.

[50] W. M. Rohsenow and H. Choi, *Heat, Mass, and Momentum Transfer*, Prentice Hall, London, 1961.

[51] T. Kenichiro, N. Takabumi, M. Masaaki, T. Ayao, and F. Tetsuro, "Experimental study on combined forced and natural convection heat transfer in an isothermally heated vertical parallel plates," in *Proceedings of National Heat Transfer Symposium*, pp. 127–129, Japan, 1984.

[52] P. A. Weiss and R. J. Hertlein, "UPTF test results: first three separate effect tests," *Nuclear Engineering and Design*, vol. 108, no. 1-2, pp. 249–263, 1988.

[53] W. H. McAdams, *Heat Transmission*, McGraw-Hil, New York (United States), 1954.

[54] D. L. Selby, *Pressurized thermal shock evaluation of the H. B. Robinson Unit 2 Nuclear Power Plant (Appendices A-K), Volume 2, NUREG/CR-4183-Vol. 2*, ORNL/TM-9567/V2, United States, 1985.

[55] P. M. Brdlik, I. P. Semenov, and B. N. Kovalev, "Heat transfer investigation for mixed free and forced turbulent convection on vertical plate," in *Symposium on Turbulent Shear Flows, Imperial College of Science and Technology*, pp. 9.35–9.40, London, England, 1979.